nature sustainability

Article

https://doi.org/10.1038/s41893-023-01132-6

Quantifying the human cost of global warming

Received: 25 July 2022

Accepted: 20 April 2023

Published online: 22 May 2023

Check for updates

Timothy M. Lenton[1,9] ✉, Chi Xu[2,9] ✉, Jesse F. Abrams[1], Ashish Ghadiali[1], Sina Loriani[3], Boris Sakschewski[3], Caroline Zimm[4], Kristie L. Ebi[5], Robert R. Dunn[6], Jens-Christian Svenning[7] & Marten Scheffer[8]

The costs of climate change are often estimated in monetary terms, but this raises ethical issues. Here we express them in terms of numbers of people left outside the 'human climate niche'—defined as the historically highly conserved distribution of relative human population density with respect to mean annual temperature. We show that climate change has already put ~9% of people (>600 million) outside this niche. By end-of-century (2080–2100), current policies leading to around 2.7 °C global warming could leave one-third (22–39%) of people outside the niche. Reducing global warming from 2.7 to 1.5 °C results in a ~5-fold decrease in the population exposed to unprecedented heat (mean annual temperature ≥29 °C). The lifetime emissions of ~3.5 global average citizens today (or ~1.2 average US citizens) expose one future person to unprecedented heat by end-of-century. That person comes from a place where emissions today are around half of the global average. These results highlight the need for more decisive policy action to limit the human costs and inequities of climate change.

Despite increased pledges and targets to tackle climate change, current policies still leave the world on course for around 2.7 °C end-of-century global warming[1–5] above pre-industrial levels—far from the ambitious aim of the Paris Agreement to limit global warming to 1.5 °C. Even fully implementing all 2030 nationally determined contributions, long-term pledges and net zero targets, nearly 2 °C global warming is expected later this century[1,2,5]. Calls for climate justice highlight the vital need to address the social injustices driven by climate change[6]. But what is the human cost of climate change and who bears it? Existing estimates tend to be expressed in monetary terms[7], tend to recognize impacts on the rich more than those on the poor (because the rich have more money to lose) and tend to value those living now over those living in the future (because future damages are subject to economic discounting). From an equity standpoint, this is unethical[8]—when life or health are at stake, all people should be considered equal, whether rich or poor, alive or yet to be born.

A growing body of work considers how climate variability and climate change affect morbidity[9] or mortality[10–13]. Here, we take a complementary, ecological approach, considering exposure to less favourable climate conditions, defined as deviations of human population density with respect to climate from the historically highly conserved distribution—the 'human climate niche'[14]. The climate niche of species integrates multiple causal factors including combined[15] effects of physiology[16] and ecology[17]. Humans have adapted physiologically and culturally to a wide range of local climates, but despite this our niche[14] shows a primary peak of population density at a mean annual temperature (MAT) of ~13 °C and a secondary peak at ~27 °C (associated with monsoon climates principally in South Asia). The density of domesticated crops and livestock follow similar distributions[14], as does

[1]Global Systems Institute, University of Exeter, Exeter, UK. [2]School of Life Sciences, Nanjing University, Nanjing, China. [3]Potsdam Institute for Climate Impact Research, Potsdam, Germany. [4]International Institute for Applied Systems Analysis, Laxenburg, Austria. [5]Center for Health and the Global Environment, University of Washington, Seattle, WA, USA. [6]Department of Applied Ecology, North Carolina State University, Raleigh, NC, USA. [7]Center for Biodiversity Dynamics in a Changing World (BIOCHANGE) and Section for Ecoinformatics and Biodiversity, Department of Biology, Aarhus University, Aarhus, Denmark. [8]Wageningen University, Wageningen, The Netherlands. [9]These authors contributed equally: Timothy M. Lenton, Chi Xu.
✉e-mail: t.m.lenton@exeter.ac.uk; xuchi@nju.edu.cn

https://doi.org/10.1038/s41893-023-01132-6

gross domestic product, which shares the same independently identified[14,18] primary temperature peak (~13 °C). Mortality also increases at both high and low temperatures[10–12], consistent with the existence of a niche.

Here, we reassess the human climate niche, review its mechanistic basis, link it to temperature extremes, and calculate exposure outside the niche up to present and into the future under different demographic scenarios and levels of global warming. Exposure outside the niche could result in increased morbidity, mortality, adaptation in place or displacement (migration elsewhere). High temperatures have been linked to increased mortality[12,13], decreased labour productivity[19], decreased cognitive performance[20], impaired learning[21], adverse pregnancy outcomes[22], decreased crop yield potential[9], increased conflict[23–25], hate speech[26], migration[27] and infectious disease spread[9,28,29]. Climate-related sources of harm not captured by the niche include sea-level rise[30,31].

Reassessing the niche

First, we re-examined how relative population density varies with MAT. Our previous work[14] considered the 2015 population distribution under the 1960–1990 mean climate as a baseline (Extended Data Fig. 1). Here, we use the 1980 population distribution (total 4.4 billion) under the 1960–1990 mean climate (Fig. 1a; '1980') as the reference state. This is a more internally consistent approach, particularly as recent population growth biases towards hotter places. Applying a double-Gaussian fitting, the primary temperature peak is now larger and at a slightly lower temperature (~12 °C), in better agreement with reconstructions from 300, 500 and 6,000 years BP (Extended Data Fig. 1). The 1960–1990 interval was globally ~0.3 °C warmer than the 1850–1900 'pre-industrial' level, but closer to mean Holocene temperatures that supported civilizations as we know them (because 1850–1900 was at the end of the Little Ice Age). The smoothed double-Gaussian function fit (Fig. 1a; '1980 fitted') is referred to from hereon as the 'temperature niche'. An updated 'temperature–precipitation niche' (additionally considering mean annual precipitation; MAP) was also calculated and considered in sensitivity analyses. It shows a marked drop in population density[14,32] below 1,000 mm yr^{-1} MAP. The temperature niche captures a key part of this effect because its minimum at 19–24 °C is associated with dry subtropical climates (Extended Data Fig. 2). However, the temperature niche overestimates population density at very low MAP (notably in temperate deserts) and at high MAP (Supplementary Fig. 1). Hence, projections with the temperature niche are more conservative than those with the temperature–precipitation niche. By either definition, the niche is largely that of people dependent on farming. The niche of hunter-gatherers is probably broader[33–36], as it is not constrained by the niches of domesticated species. This hypothesis is supported by the broader distribution of population density with respect to temperature reconstructed[14] from the ArchaeoGLOBE dataset for 6,000 years BP (when a smaller fraction of total population depended on farming; Extended Data Fig. 1b).

Mechanisms behind the niche

The human climate niche is shaped by direct effects of climate on us and indirect effects on the species and resources that sustain or afflict us. Direct climate effects include health impacts and changes in behaviour. Human perceptions of thermal comfort evolved[37] to keep us near optimal conditions of 22–26 °C, with well-being declining[38] above 28 °C. Behavioural changes include altering clothing, changing environment (including to indoor environments) and altering work patterns[39]. These can buffer individual exposure to temperature extremes but still affect collective well-being via effects on work. Sometimes uncomfortable conditions are unavoidable. High temperatures can decrease labour productivity[19], cognitive performance[20] and learning[21], produce adverse pregnancy outcomes[22], and increase mortality[10–12]. Exposure to temperatures >40 °C can be lethal[40], and lethal temperature decreases as humidity increases[12,40]. At wet-bulb temperature (WBT) >28 °C, the effectiveness of sweating in cooling the body decreases, and WBT ~35 °C can be fatal[41,42] especially for more vulnerable individuals[43] (as the body can no longer cool itself). High temperatures can also trigger conflict[23–25] or migration[27] to lower temperature locations.

Indirect effects of climate occur where climate influences the distribution and abundance of species or resources that sustain or afflict humans. Warmer, wetter conditions tend to favour vectors of human

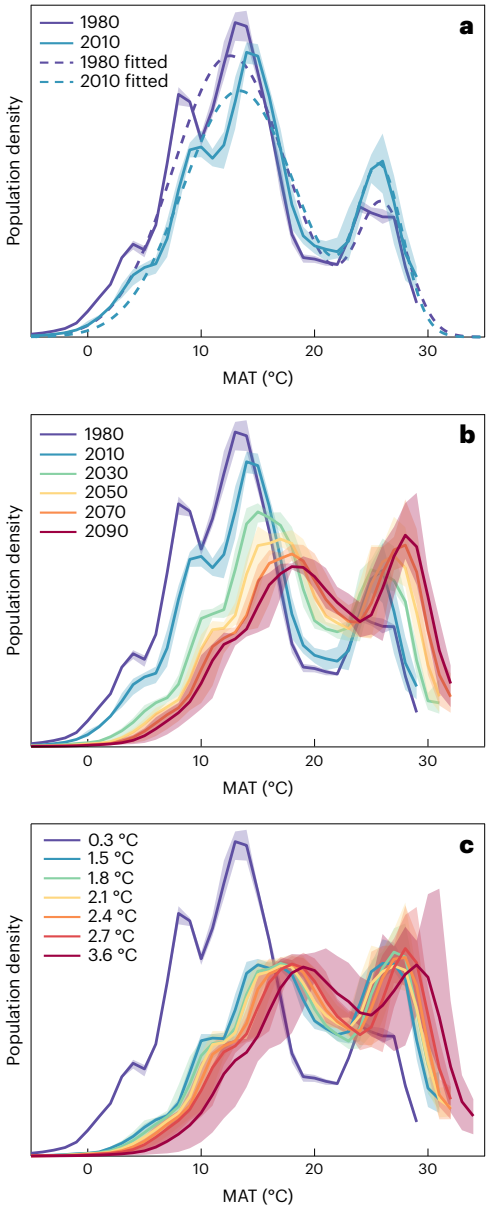

Fig. 1 | Changes in relative human population density with respect to MAT. **a**, Observed changes from the reference distribution for 1980 population (4.4 billion) under 1960–1990 climate (0.3 °C global warming), to the 2010 population (6.9 billion) under 2000–2020 climate (1.0 °C global warming), together with smooth fitted functions ('1980 fitted' is defined as the temperature niche). **b**, Observed and projected future changes in population density with respect to MAT following SSP2-4.5 leading to ~2.7 °C global warming and peak population 9.5 billion (see Extended Data Table 1 for global warming and population levels at each time). **c**, Projected population density with respect to MAT for a future world of 9.5 billion people under different levels of global warming (1.5, 1.8, 2.1, 2.4, 2.7 and 3.6 °C), contrasted with the reference distribution (0.3 °C, 1980 population). Data are presented as mean values with the shaded regions corresponding to 5th–95th percentiles.

disease[9,28,29,44]. The majority of the world's population remains directly dependent on access to freshwater and lives within 3 km of a surface freshwater body[14,32,45]. Around 2 billion people depend on subsistence agriculture and thus the climate niche(s) of their crops. A further 120 million pastoralists depend on their domesticated animals, which as mammals have similar physiological limits to humans[40,46]. Despite a globalized food market, most countries pursue food security through localized production. This couples the rest of us to the climate niches of the crops and livestock we consume, which are similar to the niche of humans[14]. High temperatures decrease crop yield potential[9] and warming is spreading key crop pests and pathogens[47,48]. Major rainfed crops (maize, rice, wheat) are already migrating[49], somewhat mitigated by increases in irrigation[49]. This and the historical constancy of the niche (Extended Data Fig. 1a) suggest technological advancement has limited potential to expand the human climate niche in future.

Calculating exposure

For projections, we assume the temperature niche remains unaltered, and provide three calculations of exposure outside of it: (1) exposure to unprecedented heat; (2) total exposure due to temperature change only; or (3) total exposure due to temperature and demographic change (see Methods). (1) The simplest approach[14] just considers 'hot exposure'—that is, how many people fall outside the hot edge of the temperature niche. This is calculated[14] for a given climate and population distribution as the percentage of population exposed to MAT ≥29 °C, given that only 0.3% of the 1980 population (12 million) experienced such conditions in the 1960–1990 climate. (2) Total exposure due to temperature change alone[14] considers all areas where temperature increases to a value supporting lower relative population density according to the temperature niche. To calculate this[14] (Extended Data Fig. 3), we apply the niche to create a spatial 'ideal distribution' of relative population density under a changed climate that maintains the historical distribution with respect to temperature. This is contrasted with the spatial 'reference distribution' of population density with respect to the 1960–1990 climate. The difference between the two distributions integrated across space gives the percentage of population exposed outside the niche due to climate only. (3) Demographic change can also expose an increased density of population to a less favourable climate. To provide an upper estimate of population exposure (in %) due to both temperature and demographic change (Extended Data Fig. 3), we integrate the difference between the projected spatial 'assumed distribution' of population density with respect to temperature and the 'ideal distribution'.

Linking average temperature to other thermal metrics

MAT has the advantage of data availability for characterizing and projecting the human climate niche—it can be easily derived from observational data, reanalysis or climate model output. However, other metrics with less available data have been proposed to better capture thermal tolerance of humans, including mean maximum temperature[46] (MMT) and WBT[40]. Reassuringly, we find that MAT is very highly correlated with both annual MMT and mean annual WBT (Supplementary Fig. 2). Given the importance of extremes, we also considered how the number of days with maximum temperature >40 °C or with WBT >28 °C varies with MAT (Extended Data Fig. 4). Potentially lethal[40] exposure to maximum temperature >40 °C starts to increase markedly above MAT ~27 °C, reaching an average of over 75 days a year at MAT ~29 °C (half the longest time experienced in the present world), and almost all locations with MAT ≥29 °C experience a substantial number of days with maximum temperature >40 °C (Extended Data Fig. 4a). Physiologically challenging exposure to WBT >28 °C starts to increase at MAT >22 °C and exceeds an average of 10 days per year at MAT ≥29 °C (Extended Data Fig. 4b). Together these results show that MAT provides a good proxy for characterizing thermal tolerance, with MAT ≥29 °C providing a reasonable measure of unprecedented heat exposure, although it does not capture all exposure to temperature extremes.

Changes up to present

We find that noticeable changes in the distribution of population density with respect to temperature have occurred due to temperature and demographic changes from 1980 to 2010 (Fig. 1a). Considering the 2010 population distribution (total 6.9 billion) under the observed 2000–2020 climate, global warming of 1.0 °C (0.7 °C above 1960–1990) has shifted the primary peak of population density to a slightly higher temperature (~13 °C) compared with 1980, and the bias of population growth towards hot places has the increased population density at the secondary (~27 °C) peak. Greater observed global warming in the cooler higher northern latitudes than the tropics is visible in the changes to the distribution (Fig. 1a). Hot exposure (MAT ≥29 °C) tripled in percentage terms to 0.9 ± 0.4% (mean ± s.d.; 62 ± 26 million people), 9 ± 1% of the global population have been exposed outside the niche due to temperature change alone and 10 ± 1% from temperature plus demographic change (Fig. 2). Thus, global warming of 0.7 °C since 1960–1990 has put 624 ± 70 million people in less favourable temperature conditions, with demographic change adding another 77 million.

Future exposure

To estimate future exposure, we use an ensemble of eight climate model outputs (Supplementary Table 1) and corresponding population projections from four Shared Socioeconomic Pathways[50] (SSPs; Extended Data Table 1)—scenarios of socioeconomic global changes and associated greenhouse gas emissions up to 2100. The 'middle of the road' (SSP2-4.5) pathway provides a useful reference scenario because it produces end-of-century (2081–2100) average global warming of 2.7 (range 2.1–3.5) °C corresponding to the 2.7 (2.0–3.6) °C expected under current policies[1], and it captures population growth towards a peak of ~9.5 billion in 2070 (then declining to ~9.0 billion in 2100). Global warming and population growth combine to shift relative population density to higher temperature (Fig. 1b). Hot exposure (Fig. 2a,d) becomes significant by 2030 at 4 ± 2% or 0.3 ± 0.1 billion as global warming reaches 1.5 °C, and it increases near linearly to 23 ± 9% or 2.1 ± 0.8 billion in 2090 under 2.7 °C global warming. The number of people left outside the niche due to temperature change alone (Fig. 2b,e) reaches 14 ± 3% or 1.2 ± 0.2 billion by 2030, more than doubling to 29 ± 5% or 2.7 ± 0.5 billion in 2090. The number of people left outside the niche from temperature plus demographic change (Fig. 2c,f) reaches 25 ± 2% or 2.0 ± 0.2 billion by 2030, and 40 ± 4% or 3.7 ± 0.4 billion by 2090.

Variation across the SSPs

The other three SSPs produce a wide range of global warming (2081–2100) from ~1.8 (1.3–2.4) °C to ~4.4 (3.3–5.7) °C and span a wide range of human development trajectories, from population peaking at ~8.5 billion then declining to ~6.9 billion in 2100 to ongoing growth to ~12.6 billion in 2100 (Extended Data Table 1). Both global warming and demographic change alter the distribution of relative population density with respect to temperature (Extended Data Fig. 5). By 2090, hot exposure reaches 8–40% or 0.6–4.7 billion across scenarios (Fig. 2a,d). The number of people left outside the niche due to temperature change only reaches 18–47% or 1.3–4.7 billion (Fig. 2b,e). Adding in demographic change increases this to 29–53% or 2.2–6.5 billion (Fig. 2c,f). Estimates of exposure outside the combined temperature–precipitation niche are roughly 20% greater than for the temperature niche alone (Extended Data Fig. 6). The 'fossil-fuelled development' (SSP5-8.5) pathway exposes the greatest proportion of the population to unprecedented heat or being pushed out of the niche due to climate change alone, but the 'regional rivalry' (SSP3-7.0) pathway exposes the greatest proportion of the population due to climate and demographic change combined, and the greatest absolute numbers across all three measures of exposure (Fig. 2 and Extended Data Fig. 6).

https://doi.org/10.1038/s41893-023-01132-6

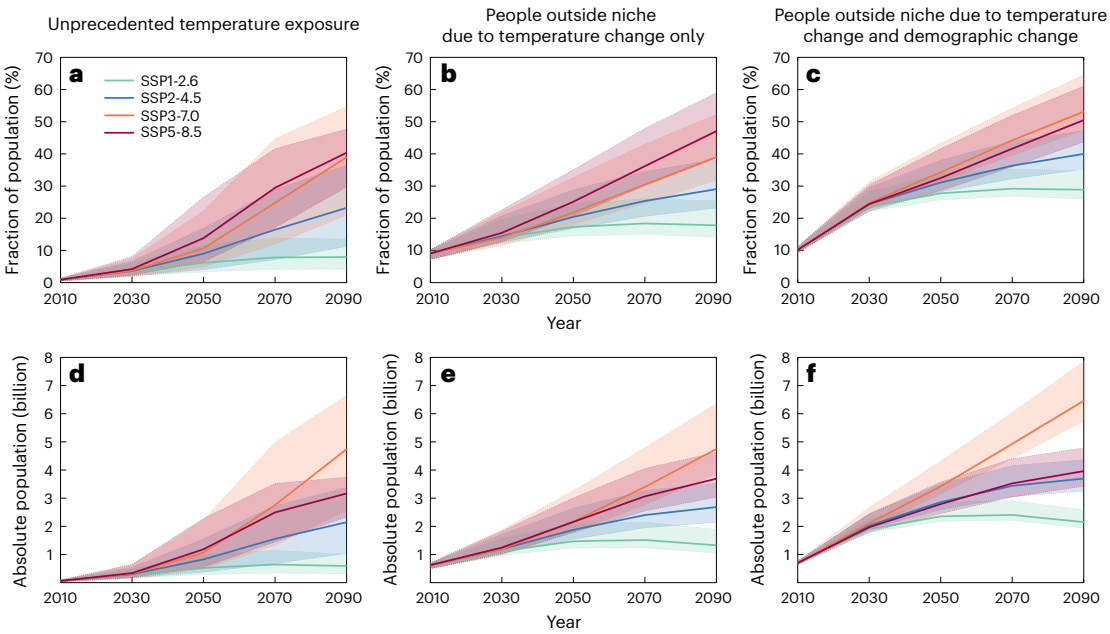

Fig. 2 | Population exposed outside of the temperature niche, following different SSPs. a–f, Fraction of population (%; **a**–**c**) and absolute population (billion people; **d**–**f**) exposed to unprecedented temperatures (MAT ≥29 °C; **a**,**d**), left outside the niche due to temperature change only (**b**,**e**,) and left outside the niche due to temperature change and demographic change (**c**,**f**) for different SSPs. Calculations are based on MAT averaged over the 20-year intervals and population density distribution at the centre year of the corresponding intervals. Data are presented as mean values with the shaded regions corresponding to the 5th–95th percentiles.

Controlling for demography

Larger global populations following the SSPs place a greater proportion of people in hotter places, tending to leave more outside the niche (irrespective of global warming). To isolate the effects of climate policy and associated climate change on exposure, we fix the population and its distribution, exploring three different options: (1) 6.9 billion (as in 2010); (2) 9.5 billion (as in SSP2 in 2070); and (3) 11.1 billion (as in SSP3 in 2070). Having controlled for demography, global warming shifts the whole distribution of population density to higher temperatures (Fig. 1c and Extended Data Fig. 7). This results in linear relationships (Fig. 3) between global warming and the percentage of the population exposed to unprecedented heat or left outside the niche from temperature change only, or temperature change plus demographic change. Hot exposure (Fig. 3a) starts to become significant above the present level of ~1.2 °C global warming and increases steeply at 11.9 % $°C^{-1}$ (6.9 billion) to 17.5 % $°C^{-1}$ (11.1 billion). Exposure due to temperature change alone increases 11.8 % $°C^{-1}$ above the baseline defined at 0.3 °C global warming (1960–1990; Fig. 3b). Factoring in demography, for a greater fixed population, the percent exposed is always greater, but the dependence on climate weakens somewhat towards 9.1 % $°C^{-1}$ (for 11.1 billion). The relationships between global warming and exposure are all steeper for the temperature–precipitation niche (Extended Data Fig. 8a). The mean temperature experienced by an average person increases with global warming in a manner invariant to demography at +1.5 °C $°C^{-1}$ (Extended Data Fig. 8b), consistent with observations and models that the land warms ~1.5 times faster than the global average[51].

Worst-case scenarios

We now focus on a future world of 9.5 billion. When assessing risk it is important to consider worst-case scenarios[52]. If the transient climate response to cumulative emissions is high, current policies could, in the worst case, lead to ~3.6 °C end-of-century global warming[1] (as projected under SSP3-7.0; Extended Data Table 1). This results in 34 ± 10% (3.3 ± 0.9 billion) hot exposed, 39 ± 7% (3.7 ± 0.7 billion) left outside the niche from temperature change only and 48 ± 7% (4.5 ± 0.6 billion) when including demographic change (Fig. 3). There also remains the possibility that climate policies are not enacted, and the world reverts to fossil-fuelled development (SSP5-8.5), leading to ~4.4 °C end-of-century global warming. This gives 45 ± 7% (4.2 ± 0.7 billion) hot exposed, 47 ± 8% (4.5 ± 0.7 billion) left outside the niche from temperature change only and 55 ± 7% (5.3 ± 0.6 billion) when including demographic change (Fig. 3).

Gains from strengthening climate policy

Having controlled for demography, strengthening climate policy reduces exposure (Figs. 1c and 3), including to unprecedented heat (Fig. 4), through reducing geographical movement of the temperature and temperature–precipitation niches (Extended Data Fig. 9). Following Climate Action Tracker's November 2021 projections[1], different levels of policy ambition result in ~0.3 °C changes in end-of-century global warming as follows: current policies lead to ~2.7 (2.0–3.6) °C; meeting current 2030 nationally determined contributions (without long-term pledges) leads to ~2.4 (1.9–3.0) °C; additional full implementation of submitted and binding long-term targets leads to ~2.1 (1.7–2.6) °C; and fully implementing all announced targets leads to ~1.8 (1.5–2.4) °C. Overall, going from ~2.7 °C global warming under current policies to meeting the Paris Agreement 1.5 °C target reduces hot exposure from 22 to 5% (2.1 to 0.4 billion; Fig. 3a). It reduces population left outside the niche due to temperature change only from 29 to 14% (2.8 to 1.3 billion) and it reduces population left outside the niche by temperature plus demographic changes from 39 to 28% (3.7 to 2.7 billion; Fig. 3b). Thus, each 0.3 °C decline in end-of-century warming reduces hot exposure by 4.3% or 410 million people, it reduces population left outside the niche due to temperature change only by 3.7% or 350 million people, and population left outside the niche due to temperature and demographic changes by 2.8% or 270 million people.

Country-level exposure

We focus on hot exposure as the simplest and most conservative metric. The population exposed to unprecedented heat (MAT ≥29 °C)

https://doi.org/10.1038/s41893-023-01132-6

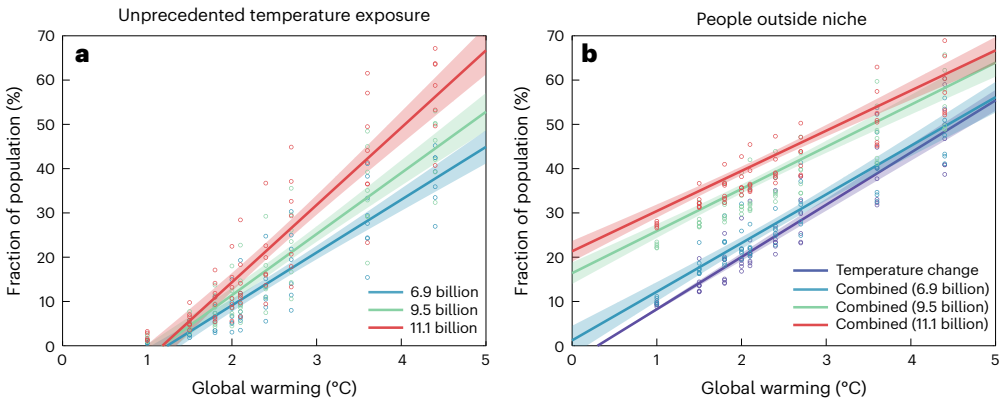

Fig. 3 | Relationships between global warming and population exposed outside the temperature niche for different fixed population distributions. **a**, Population (%) exposed to unprecedented heat (MAT ≥29 °C) for the different population distributions: 6.9 billion (blue; $n = 65$, coefficient = 11.9 % °C^{-1}, $r^2 = 0.83$); 9.5 billion (green; $n = 65$, coefficient = 13.8 % °C^{-1}, $r^2 = 0.83$); and 11.1 billion (red; $n = 65$, coefficient = 17.5 % °C^{-1}, $r^2 = 0.83$). **b**, Population (%) exposed outside the temperature niche due to temperature change only (purple; $n = 65$, coefficient = 11.8 % °C^{-1}, forcing intercept at 1960–1990 global warming of 0.3 °C), and due to the combined effects of temperature change and demographic change, for different fixed population distributions: 6.9 billion in 2010 (blue; $n = 65$, coefficient = 11.0 % °C^{-1}, $r^2 = 0.83$); 9.5 billion following SSP2 in 2070 (green; $n = 65$, coefficient = 9.5 % °C^{-1}, $r^2 = 0.84$); and 11.1 billion following SSP3 in 2070 (red; $n = 65$, coefficient = 9.1 % °C^{-1}, $r^2 = 0.84$). The shaded regions correspond to 95% two-sided confidence intervals of the estimated regression coefficients.

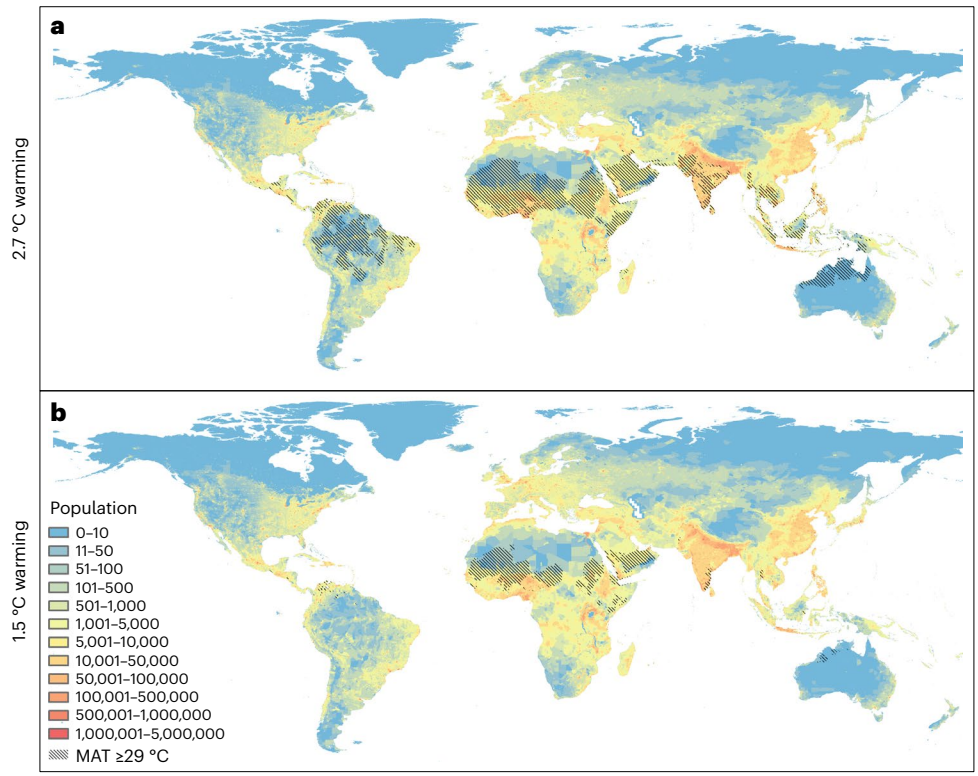

Fig. 4 | Regions and population densities exposed to unprecedented heat at different levels of global warming. a,**b**, Regions exposed to unprecedented heat (MAT ≥29 °C) overlaid on population density (number in a ~100 km^2 grid cell) for a world of 9.5 billion (SSP2, 2070) under 2.7 °C global warming (**a**) and 1.5 °C global warming (**b**).

worldwide declines ~5-fold if global warming is reduced from ~2.7 °C under current policies to meeting the 1.5 °C target (Fig. 5a and Supplementary Data). Assuming a future world of 9.5 billion, India has the greatest population exposed under 2.7 °C global warming, >600 million, but this reduces >6-fold to ~90 million at 1.5 °C global warming. Nigeria has the second largest population exposed, >300 million under 2.7 °C global warming, but this reduces >7-fold to <40 million at 1.5 °C global warming. For third-ranked Indonesia, hot exposure reduces >20-fold, from ~100 million under 2.7 °C global warming to <5 million at 1.5 °C global warming. For fourth- and fifth-ranked Philippines and Pakistan with >80 million exposed under 2.7 °C global warming, there are even larger proportional reductions at 1.5 °C global warming. Sahelian–Saharan countries including Sudan (sixth ranked) and Niger (seventh) have a ~2-fold reduction in exposure, because they still have a large fraction of land area hot exposed at 1.5 °C global warming (Fig. 5b). The fraction of land area exposed approaches 100% for several countries under 2.7 °C global warming (Fig. 5b). Brazil has the greatest absolute land area exposed under 2.7 °C global warming,

https://doi.org/10.1038/s41893-023-01132-6

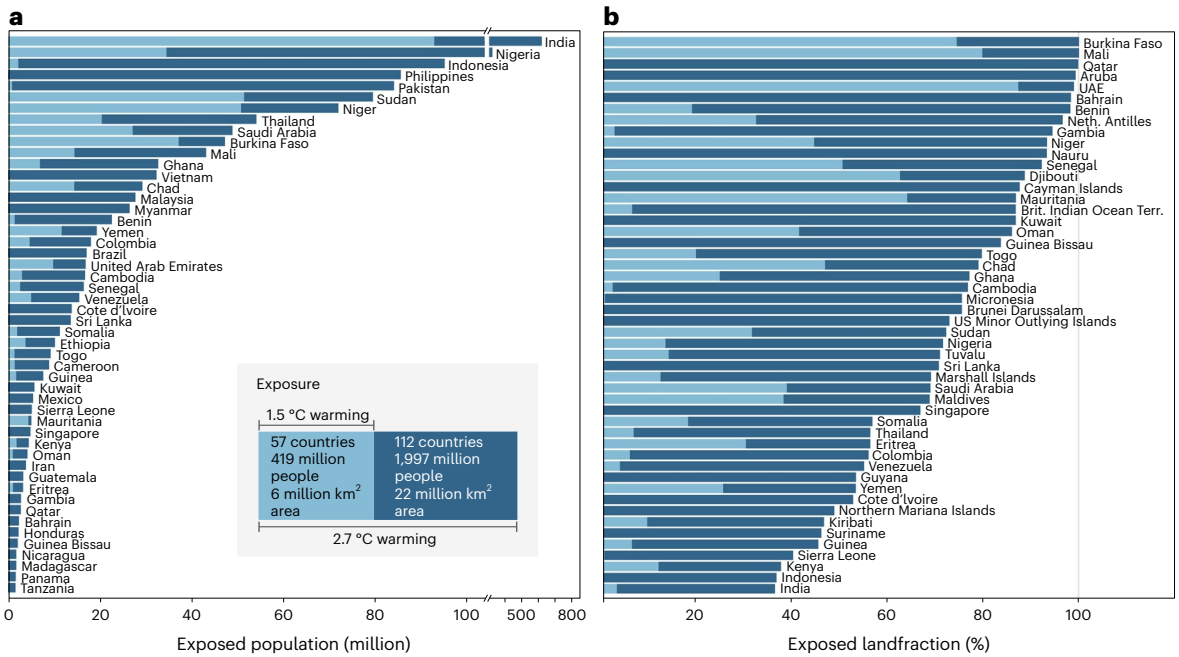

Fig. 5 | Country-level exposure to unprecedented heat (MAT ≥29 °C) at 2.7 °C and 1.5 °C global warming in a world of 9.5 billion people (around 2070 under SSP2). a, Population exposed for the top 50 countries ranked under 2.7 °C global warming (dark blue) with exposure at 1.5 °C global warming overlaid (pale blue). Note the break in the *x* axis for the top two countries. **b**, Fraction of land area exposed for the top 50 countries (again ranked under 2.7 °C global warming with results for 1.5 °C global warming overlaid). The inset in **a** summarizes the total global exposure of countries, population and land area at the two levels of global warming, with results for all countries provided in Supplementary Data. UAE, United Arab Emirates; Neth. Antilles, Netherlands Antilles; Brit. Indian Ocean Terr., British Indian Ocean Territory.

despite almost no area being exposed at 1.5 °C, and Australia and India also experience massive increases in absolute area exposed (Fig. 4). (If the future population reaches 11.1 billion, the ranking of countries by population exposed remains similar, although the numbers exposed increase.) Those most exposed under 2.7 °C global warming come from nations that today are above the median poverty rate and below the median per capita emissions (Fig. 6).

Relating present emissions to future exposure

Above the present level of 1.2 °C global warming, the increase in hot exposure of 13.8% $°C^{-1}$ for a future world of ~9.5 billion people (cap.; Fig. 3a), corresponds to 1.31×10^9 cap. $°C^{-1}$. The established relationship[53] of cumulative emissions (EgC) to transient global warming is ~1.65 (1.0–2.3) °C EgC^{-1}. Therefore one person will be exposed to unprecedented heat (MAT ≥29 °C) for every ~460 (330–760) tC emitted. Present (2018 data) global mean per capita CO_2-equivalent (C_{eq}) emissions[54] (production-based) are 1.8 tC_{eq} $cap.^{-1}$ yr^{-1}. Thus, during their lifetimes (72.6 years) ~3.5 global average citizens today (less than the average household of 4.9 people) emit enough carbon to expose one future person to unprecedented heat. Citizens in richer countries generally have higher emissions[54], for example, the European Union (2.4 tC_{eq} $cap.^{-1}$ yr^{-1}), the USA (5.3 tC_{eq} $cap.^{-1}$ yr^{-1}) and Qatar (18 tC_{eq} $cap.^{-1}$ yr^{-1}; Fig. 6), and consumption-based emissions are even higher. Thus, ~2.7 average European Union citizens or ~1.2 average US citizens emit enough carbon in their lifetimes to expose one future person to unprecedented heat, and the average citizen of Qatar emits enough carbon in their lifetime to expose ~2.8 future people to unprecedented heat. Those future people tend to be in nations that today have per capita emissions around the 25% quantile (Fig. 6), including the two countries with the greatest population exposed: India (0.73 tC_{eq} $cap.^{-1}$ yr^{-1}) and Nigeria (0.55 tC_{eq} $cap.^{-1}$ yr^{-1}). We estimate that the average future person exposed to unprecedented heat comes from a place where today per capita emissions are approximately half (56%) of the global average (or 52% in a world of 11.1 billion people).

Discussion

Our estimate that global warming since 1960–1990 has put more than 600 million people outside the temperature niche is consistent with attributable impacts of climate change affecting 85% of the world's population[55]. Above the present level of ~1.2 °C global warming, exposure to unprecedented average temperatures (MAT ≥29 °C) is predicted to increase markedly (Fig. 3a), increasing exposure to temperature extremes (Extended Data Fig. 4). This is consistent with extreme humid heat having more than doubled in frequency[42] since 1979, associated with labour loss of 148 million full-time equivalent jobs[19], with exposure in urban areas increasing for 23% of the world's population[56] from 1983 to 2016 (due also to growing urban heat islands) and the total urban population exposed tripling[56] (due also to demographic change). Both India and Nigeria already show 'hotspots' of increased exposure to extreme heat due predominantly to warming[56], consistent with our prediction that they are at greatest future risk (Fig. 5). These and other emerging economies (for example, Indonesia, Pakistan, Thailand) dominate the total population exposed to unprecedented heat in a 2.7 °C warmer world (Fig. 5). Their climate policy commitments also play a significant role in determining end-of-century global warming[5].

The huge numbers of humans exposed outside the climate niche in our future projections warrant critical evaluation. Combined effects of temperature and demographic change are upper estimates. This is because at any given time the method limits absolute population density of the (currently secondary) higher-temperature peak based on absolute population density of the (currently primary) lower-temperature peak. Yet absolute population density is allowed to vary (everywhere) over time. (This is not an issue for the temperature change only or hot exposure estimates.) Nevertheless, a bias of population growth to hot places clearly increases the proportion (as well as the absolute number) of people exposed to harm from high temperatures[57]. Colder places are projected to become more habitable (Extended Data Fig. 9) but are not where population growth is concentrated.

https://doi.org/10.1038/s41893-023-01132-6

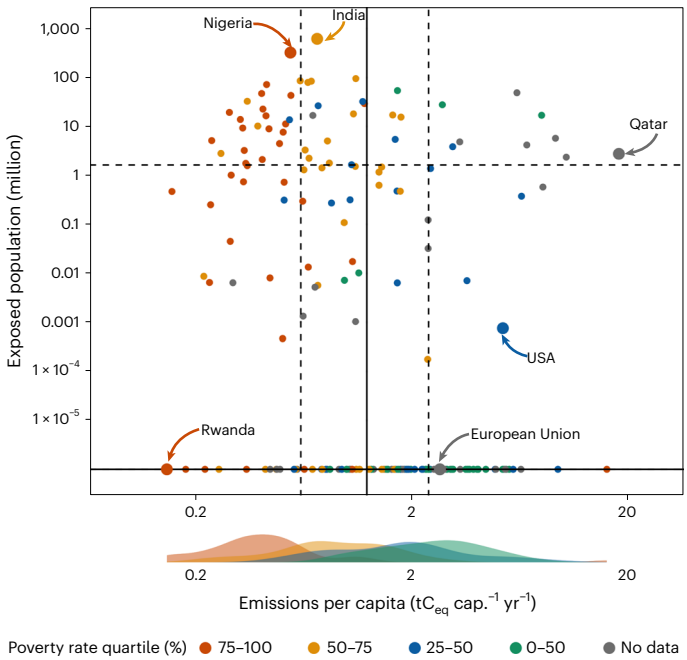

Fig. 6 | Country-level per capita greenhouse gas emissions[54] related to population exposed to unprecedented heat (MAT ≥29 °C) at 2.7 °C global warming (Fig. 5a) and poverty rate[80]. Solid lines show the median (50% quantile) and dashed lines show the 25% and 75% quantiles for emissions and heat exposure. Points are coloured by quartile of the poverty rate distribution, where poverty rate is defined as the percentage of national population below the US$1.90 poverty line. The density plots at the bottom show the distribution of emissions per capita for each poverty rate quartile.

Nor do we consider exposure to other sources of climate harm there (or elsewhere), including sea-level rise[30,31], increasing climate extremes[58] and permafrost thaw[59].

Overall, our results illustrate the huge potential human cost and the great inequity of climate change, informing discussions of loss and damage[60,61]. The worst-case scenarios of ~3.6 °C or even ~4.4 °C global warming could put half of the world population outside the historical climate niche, posing an existential risk. The ~2.7 °C global warming expected under current policies puts around a third of the world population outside the niche. It exposes almost the entire area of some countries (for example, Burkina Faso, Mali) to unprecedented heat, including some Small Island Developing States (for example, Aruba, Netherlands Antilles; Fig. 5b)—a group with members already facing an existential risk from sea-level rise. The gains from fully implementing all announced policy targets and limiting global warming to ~1.8 °C are considerable, but would still leave nearly 10% of people exposed to unprecedented heat. Meeting the goal of the Paris Agreement to limit global warming to 1.5 °C halves exposure outside the temperature niche relative to current policies and limits those exposed to unprecedented heat to 5% of people. This still leaves several least-developed countries (for example, Sudan, Niger, Burkina Faso, Mali) with large populations exposed (Fig. 5a), adding adaptation challenges to an existing climate investment trap[62]. Nevertheless, our results show the huge potential for more decisive climate policy to limit the human costs and inequities of climate change.

Methods

Reassessing the climate niche

We plot the running mean of population density against MAT, with a step of 1 °C and a bin size of 2 °C, and then apply double-Gaussian fitting to the resulting curve[14]. Our previous work[14] assessed the human temperature niche by quantifying the 2015 population distribution in relation to the 1960–1990 MAT (Extended Data Fig. 1; 'old reference'). Here, we re-assessed the temperature niche, changing the data to the 1980 population distribution (total 4.4 billion) under the 1960–1990 MAT, for greater internal consistency (Fig. 1a and Extended Data Fig. 1; '1980'). This is important because there has been significant population growth between 1980 and 2015 with a distinct bias to hotter places. The 1980 population distribution data were obtained from the History Database of the Global Environment (HYDE) 3.2 database[63]. The ensemble mean 1960–1990 climate and associated uncertainty (5th/95th percentiles) were calculated from three sources: (1) WorldClim v.1.4 data[64]; (2) Climate Research Unit Time Series (CRU TS) v.4.05 monthly data[65,66]; and (3) National Aeronautics and Space Administration Global Land Data Assimilation System (NASA GLDAS-2.1) 3-hourly data[67]. The revised temperature niche was compared with existing results for different historical intervals and datasets from ref. 14 (Extended Data Fig. 1). A revised temperature–precipitation niche was also calculated from both MAT and MAP, following the methods in ref. 14, but using the 1980 population distribution with the 1960–1990 mean climate.

Projecting the niche

Hot exposure is calculated (as previously[14]) for a given climate and population distribution as the percentage of people exposed to MAT ≥29 °C, from a direct spatial comparison of MAT and population distributions (without any smoothing). The MAT ≥29 °C threshold was chosen as only 0.3% of the 1980 population (12 million) experienced such conditions in the 1960–1990 climate. To separate the effects of climate and demographic changes on geographic displacement of the temperature niche (or the temperature–precipitation niche), we consider the following (Extended Data Fig. 3): (1) the geographic distribution of the reference niche ('reference distribution'); (2) projecting the reference niche function to the geographic distribution of present/future climate ('ideal distribution'); and (3) the geographically projected 'assumed distribution' of present/future population with respect to present/future climate conditions. Here, (2) minus (1) gives the effect of climate change only (as previously[14]), and (3) minus (2) gives the combined effect of climate and demographic change.

Linking average temperature to other thermal metrics

We assessed the relationships between MAT and other thermal metrics proposed to better capture thermal tolerance of humans, focusing on the recent interval 2000–2020. The correlations between MAT and annual MMT or mean annual WBT were assessed using linear regression with the ordinary least square method. MMT was calculated from the fifth generation European Centre for Medium-Range Weather Forecasts (ECMWF) reanalysis (ERA5) daily data at ~10 km spatial resolution and CRU TS v.4.06 monthly data at 0.5° spatial resolution. Mean annual WBT was calculated from ERA5 using the 'one-third rule' approximation based on a weighted average of dry-bulb and dewpoint temperatures[68] (this is reasonable for the annual average but overestimates daily maximum WBT). We used bias-corrected WBT[69] calculated from temperature and relative humidity data following the method of ref. 70 for six Coupled Model Intercomparison Project Phase 6 (CMIP6) models (limited to CNRM-CM6-1, CNRM-ESM2-1, CanESM5, GFDL-ESM4, MIROC-ES2L and MRI-ESM2-0 due to data availability) to derive daily maximum WBT and mean annual WBT. A model ensemble was created by resampling all model outputs to the coarsest model spatial resolution (2.8°; that of CanESM5 and GFDL-ESM4) using a bilinear interpolation method—each pixel in the resampled raster is the result of a weighted average of the nearest pixels in the original raster (this avoids biassing the ensemble towards higher resolution models). To assess the relationships between MAT and heat extremes, we considered the number of days with maximum temperature >40 °C or with WBT >28 °C. We used the ERA5 hourly data to calculate by grid point the average number of days in a year (between 2000 and 2020) with maximum dry-bulb temperature >40 °C. We used the CMIP6 model

ensemble daily maximum WBT to calculate by grid point the average number of days per year (between 2000 and 2020) with maximum WBT >28 °C. Running means were calculated with a bin width of 2 °C, a step of 0.5 °C and a minimum bin size of 20 data points.

Changes up to present

To calculate changes up to (near) present, we construct an ensemble mean 2000–2020 climate and associated uncertainty (5th/95th percentiles) from five sources: (1) CRU TS v.4.05 monthly data[65,66]; (2) NASA GLDAS-2.1 3-hourly data[67]; (3) ECMWF ERA5-Land monthly averaged climate reanalysis data[71]; (4) NASA Famine Early Warning Systems Network Land Data Assimilation System (FLDAS) monthly data[72,73]; and (5) the United States National Centers for Environmental Prediction Climate Forecast System Version 2 (NCEP CFSv2) 6-hourly data[74]. Each climate dataset is aggregated to calculate MAT and precipitation. The 2000–2020 climate represents 1.0 °C global warming relative to the pre-industrial level. The 2010 population distribution data was obtained from the HYDE 3.2 database[63]. We followed the methods described above to calculate exposure.

Future projections

We used projected climate and population distribution under four different SSPs, which combine different demographic[75] and emissions projections under consistent storylines: SSP1-2.6 (sustainability), SSP2-4.5 (middle of the road), SSP3-7.0 (regional rivalry) and SSP5-8.5 (fossil-fuelled development). We focused on 20-year mean climate states for 2020–2040, 2040–2060, 2060–2080 and 2080–2100, and the projected population distribution data of 2030, 2050, 2070 and 2090, to represent average demographic conditions of corresponding time periods (Extended Data Table 1). We obtained downscaled CMIP6 climate data available from WorldClim v.2.0 at 0.0833° (~10 km) resolution, which restricts us to up to eight CMIP6 models: BCC-CSM2-MR, CNRM-CM6-1, CNRM-ESM2-1, CanESM5, GFDL-ESM4, IPSL-CM6A-LR, MIROC-ES2L and MRI-ESM2-0 (Supplementary Table 1). We obtained SSP population projection data at 1 km resolution from the spatial population scenarios dataset[76,77]. The SSP population projections were derived at national level using methods of multi-dimensional mathematical demography[75]. Alternative assumptions on future fertility, mortality, migration and educational transitions align to the SSP storylines on future development[78] (and exclude climate-induced migration). Spatially explicit data in line with those country-level projections were derived at 1/8° resolution using a parameterized gravity-based downscaling model[76], and further downscaled to 1 km resolution[77]. We aggregated this population data to a consistent resolution of 0.0833° (~10 km) to match the climate data and our previous analyses. We combine results across climate models to create a multi-model ensemble mean, and a 5–95% confidence interval, recognizing that the number of models available varies somewhat between SSPs and time-slices (Supplementary Table 1). To this end, we apply the MAT data of each climate model to plot population density against MAT and then combine the resulting curves to calculate the mean, and 5th and 95th percentiles.

Controlling for demography

To control for demography and thus isolate the effects of climate policy and associated climate change on exposure, we consider three different fixed populations and their spatial distributions: (1) 6.9 billion as in 2010; (2) 9.5 billion following SSP2 in 2070[75–77]; and (3) 11.1 billion following SSP3 in 2070[75–77]. These are combined with the observed (2000–2020) 1.0 °C global warming and with different future levels of global warming (1.5, 1.8, 2.0, 2.1, 2.4, 2.7, 3.6 and 4.4 °C) corresponding to different 20-year climate averages from different SSPs (Figs. 1c and 3, and Extended Data Fig. 7). Global warming of 1.5 °C and 2.0 °C are considered because of their relevance to the Paris Agreement. Values of 1.8, 2.1, 2.4 and 2.7 °C are chosen as best estimates of end-of-century global warming corresponding to different policy assumptions, taken from the Climate Action Tracker[1], which uses an ensemble of runs of the MAGICC6 model that, in turn, emulates different general circulation models from CMIP6. Global warming values of 3.6 and 4.4 °C are chosen as worst-case scenarios that also enable examining the shape of relationships between global warming and population exposure. Twenty-year SSP intervals corresponding to these different levels of global warming are chosen based on mean global warming levels from the CMIP6 model ensemble given in Table SPM.1 of the Sixth Assessment Report (AR6) of the Intergovernmental Panel on Climate Change[79] (IPCC). We try to match to warming in 2081–2100, but where earlier time intervals must be used this should have little effect on the results because the spatial pattern of temperature change is highly conserved on the century timescale. The different combinations are: 1.5 °C = SSP1-2.6 in 2021–2040; 1.8 °C = SSP1-2.6 in 2081–2100; 2.0 °C = SSP2-4.5 in 2041–2060; 2.1 °C = SSP3-7.0 in 2041–2060; 2.4 °C = SSP5-8.5 in 2041–2060; 2.7 °C = SSP2-4.5 in 2081–2100; 3.6 °C = SSP3-7.0 in 2081–2100; and 4.4 °C = SSP5-8.5 in 2081–2100. For the same time interval and SSP, different CMIP6 models can give different levels of global warming due to differing climate sensitivity. This is apparent in the spread of population exposure results for individual models (open circles in Fig. 3; Extended Data Fig. 8). However, we checked that global warming in the multi-model ensemble mean of the CMIP6 models we consider (Supplementary Table 1) matches that of the larger CMIP6 ensemble (Table SPM.1 of IPCC AR6).

Country-level estimates

Results for hot exposure for 2.7 °C and 1.5 °C global warming and populations of 9.5 or 11.1 billion were aggregated from the 0.0833° (~10 km) scale of the population and climate data to country scale. This summed the population in all grid cells within a country boundary where MAT ≥29 °C, using geographic information system data for country boundaries from the World Borders Dataset. For the grid cells that are intersected by a country boundary, they were associated with a country if over half the grid cell area fell within the country territory. Results for all countries are given in Supplementary Data.

Emissions and poverty rate of those exposed

Using the country-level breakdown of exposure to unprecedented heat in a 2.7 °C warmer world with 9.5 billion people (Fig. 5a and Supplementary Data), we calculated a weighted average for number of people exposed multiplied by percentage of global average emissions per capita today. This uses production-based, country-level C_{eq} greenhouse gas emissions from the emissions database for global atmospheric research[54], for which 2018 is the latest year. The calculation was also done for country-level exposure in a 2.7 °C warmer world of 11.1 billion. Consumption-based emissions (accounting for trade) tend to be lower than production-based emissions in poorer countries and higher in richer countries. This would increase the inequity already apparent in the results. We also examined poverty rate defined as the percentage of population per country below the US$1.90 poverty line, using the interpolated data for 2019 from the World Bank's Poverty and Inequality Platform[80]. The resulting distribution is heavily skewed with 25% quantile = 0.26%, 50% quantile = 1.79% and 75% quantile = 20%.

Reporting summary

Further information on research design is available in the Nature Portfolio Reporting Summary linked to this article.

Data availability

The historical and current population distribution data are available from the HYDE 3.2 database at https://landuse.sites.uu.nl/datasets/. The WorldClim v.1.4 data are available at https://doi.org/10.5061/dryad.fj6q573q7. The CRU TS v.4.05 and v.4.06 monthly data are available at https://crudata.uea.ac.uk/cru/data/hrg/. The NASA GLDAS-2.1 3-hourly data are available at https://developers.google.

com/earth-engine/datasets/catalog/NASA_GLDAS_V021_NOAH_G025_T3H. The ECMWF ERA5 daily data are available at https://developers.google.com/earth-engine/datasets/catalog/ECMWF_ERA5_DAILY. The bias-corrected WBT data are available at https://cds.climate.copernicus.eu/cdsapp#!/dataset/sis-extreme-indices-cmip6. The ECMWF ERA5-Land monthly data are available at https://developers.google.com/earth-engine/datasets/catalog/ECMWF_ERA5_LAND_MONTHLY. The NASA FLDAS monthly data are available at https://developers.google.com/earth-engine/datasets/catalog/NASA_FLDAS_NOAH01_C_GL_M_V001. The NCEP CFSv2 6-hourly data are available at https://developers.google.com/earth-engine/datasets/catalog/NOAA_CFSV2_FOR6H. The downscaled CMIP6 climate data are available from WorldClim v.2.0 at https://worldclim.org. The SSP population projection data are available at https://www.cgd.ucar.edu/iam/modeling/spatial-population-scenarios.html. The geographic information system data for country boundaries from the World Borders Dataset are available at https://thematicmapping.org/downloads/world_borders.php. The poverty data for 2019 from the World Bank's Poverty and Inequality Platform are available at https://pip.worldbank.org/home. All data generated during this study are available from https://doi.org/10.6084/m9.figshare.22650361.v1.

Code availability

Code used for the analysis is available from https://doi.org/10.6084/m9.figshare.22650760.v1.

References

1. *Climate Action Tracker: Warming Projections Global Update: November 2021* (Climate Analytics & NewClimate Institute, 2021).
2. *World Energy Outlook 2021* (International Energy Agency, 2021).
3. *Emissions Gap Report 2021: The Heat Is On—A World of Climate Promises Not Yet Delivered* (United Nations Environment Programme, 2021).
4. *Addendum to the Emissions Gap Report 2021* (United Nations Environment Programme, 2021).
5. Meinshausen, M. et al. Realization of Paris Agreement pledges may limit warming just below 2 °C. *Nature* **604**, 304–309 (2022).
6. Newell, P., Srivastava, S., Naess, L. O., Torres Contreras, G. A. & Price, R. Toward transformative climate justice: an emerging research agenda. *Wiley Interdiscip. Rev. Clim. Change* **12**, e733 (2021).
7. Nordhaus, W. D. Revisiting the social cost of carbon. *Proc. Natl Acad. Sci. USA* **114**, 1518–1523 (2017).
8. Nolt, J. Casualties as a moral measure of climate change. *Clim. Change* **130**, 347–358 (2015).
9. Watts, N. et al. The 2020 report of The *Lancet* Countdown on health and climate change: responding to converging crises. *Lancet* **397**, 129–170 (2021).
10. Guo, Y. et al. Global variation in the effects of ambient temperature on mortality: a systematic evaluation. *Epidemiology* **25**, 781–789 (2014).
11. Gasparrini, A. et al. Mortality risk attributable to high and low ambient temperature: a multicountry observational study. *Lancet* **386**, 369–375 (2015).
12. Mora, C. et al. Global risk of deadly heat. *Nat. Clim. Change* **7**, 501–506 (2017).
13. Parncutt, R. The human cost of anthropogenic global warming: semi-quantitative prediction and the 1,000-tonne rule. *Front. Psychol.* https://doi.org/10.3389/fpsyg.2019.02323 (2019).
14. Xu, C., Kohler, T. A., Lenton, T. M., Svenning, J.-C. & Scheffer, M. Future of the human climate niche. *Proc. Natl Acad. Sci. USA* **117**, 11350–11355 (2020).
15. Pörtner, H.-O. Climate impacts on organisms, ecosystems and human societies: integrating OCLTT into a wider context. *J. Exp. Biol.* https://doi.org/10.1242/jeb.238360 (2021).
16. Lutterschmidt, W. I. & Hutchison, V. H. The critical thermal maximum: history and critique. *Can. J. Zool.* **75**, 1561–1574 (1997).
17. Afkhami, M. E., McIntyre, P. J. & Strauss, S. Y. Mutualist-mediated effects on species' range limits across large geographic scales. *Ecol. Lett.* **17**, 1265–1273 (2014).
18. Burke, M., Hsiang, S. M. & Miguel, E. Global non-linear effect of temperature on economic production. *Nature* **527**, 235–239 (2015).
19. Parsons, L. A. et al. Global labor loss due to humid heat exposure underestimated for outdoor workers. *Environ. Res. Lett.* **17**, 014050 (2022).
20. Masuda, Y. J. et al. Heat exposure from tropical deforestation decreases cognitive performance of rural workers: an experimental study. *Environ. Res. Lett.* **15**, 124015 (2020).
21. Park, R. J., Behrer, A. P. & Goodman, J. Learning is inhibited by heat exposure, both internationally and within the United States. *Nat. Hum. Behav.* **5**, 19–27 (2021).
22. Chersich, M. F. et al. Associations between high temperatures in pregnancy and risk of preterm birth, low birth weight, and stillbirths: systematic review and meta-analysis. *Br. Med. J.* **371**, m3811 (2020).
23. Mares, D. M. & Moffett, K. W. Climate change and interpersonal violence: a "global" estimate and regional inequities. *Clim. Change* **135**, 297–310 (2016).
24. Hsiang, S. M., Burke, M. & Miguel, E. Quantifying the influence of climate on human conflict. *Science* **341**, 1235367 (2013).
25. Hsiang, S. M., Meng, K. C. & Cane, M. A. Civil conflicts are associated with the global climate. *Nature* **476**, 438–441 (2011).
26. Stechemesser, A., Levermann, A. & Wenz, L. Temperature impacts on hate speech online: evidence from 4 billion geolocated tweets from the USA. *Lancet Planet. Health* **6**, e714–e725 (2022).
27. Mueller, V., Gray, C. & Kosec, K. Heat stress increases long-term human migration in rural Pakistan. *Nat. Clim. Change* **4**, 182–185 (2014).
28. Cissé, G. et al. in *Climate Change 2022: Impacts, Adaptation and Vulnerability* (eds Pörtner, H.-O. et al.) 1041–1170 (IPCC, Cambridge Univ. Press, 2022).
29. Carlson, C. J. et al. Climate change increases cross-species viral transmission risk. *Nature* **607**, 555–562 (2022).
30. Neumann, B., Vafeidis, A. T., Zimmermann, J. & Nicholls, R. J. Future coastal population growth and exposure to sea-level rise and coastal flooding—a global assessment. *PLoS ONE* **10**, e0118571 (2015).
31. Hooijer, A. & Vernimmen, R. Global LiDAR land elevation data reveal greatest sea-level rise vulnerability in the tropics. *Nat. Commun.* **12**, 3592 (2021).
32. Small, C. & Cohen, J. Continental physiography, climate, and the global distribution of human population. *Curr. Anthropol.* **45**, 269–277 (2004).
33. Gavin, M. C. et al. The global geography of human subsistence. *R. Soc. Open Sci.* **5**, 171897 (2018).
34. Pitulko, V. V. et al. The Yana RHS site: humans in the Arctic before the Last Glacial Maximum. *Science* **303**, 52–56 (2004).
35. Pitulko, V., Pavlova, E. & Nikolskiy, P. Revising the archaeological record of the Upper Pleistocene Arctic Siberia: human dispersal and adaptations in MIS 3 and 2. *Quat. Sci. Rev.* **165**, 127–148 (2017).
36. Taylor, W. et al. High altitude hunting, climate change, and pastoral resilience in eastern Eurasia. *Sci. Rep.* **11**, 14287 (2021).
37. Just, M. G., Nichols, L. M. & Dunn, R. R. Human indoor climate preferences approximate specific geographies. *R. Soc. Open Sci.* **6**, 180695 (2019).
38. Cui, W., Cao, G., Park, J. H., Ouyang, Q. & Zhu, Y. Influence of indoor air temperature on human thermal comfort, motivation and performance. *Build. Environ.* **68**, 114–122 (2013).

39. Masuda, Y. J. et al. How are healthy, working populations affected by increasing temperatures in the tropics? Implications for climate change adaptation policies. *Glob. Environ. Change* **56**, 29–40 (2019).
40. Asseng, S., Spänkuch, D., Hernandez-Ochoa, I. M. & Laporta, J. The upper temperature thresholds of life. *Lancet Planet. Health* **5**, e378–e385 (2021).
41. Sherwood, S. C. & Huber, M. An adaptability limit to climate change due to heat stress. *Proc. Natl Acad. Sci. USA* **107**, 9552–9555 (2010).
42. Raymond, C., Matthews, T. & Horton, R. M. The emergence of heat and humidity too severe for human tolerance. *Sci. Adv.* **6**, eaaw1838 (2020).
43. Weitz, C. A., Mukhopadhyay, B. & Das, K. Individually experienced heat stress among elderly residents of an urban slum and rural village in India. *Int. J. Biometeorol.* **66**, 1145–1162 (2022).
44. Dunn, R. R., Davies, T. J., Harris, N. C. & Gavin, M. C. Global drivers of human pathogen richness and prevalence. *Proc. R. Soc. B* **277**, 2587–2595 (2010).
45. Kummu, M., de Moel, H., Ward, P. J. & Varis, O. How close do we live to water? A global analysis of population distance to freshwater bodies. *PLoS ONE* **6**, e20578 (2011).
46. Bennett, J. M. et al. GlobTherm, a global database on thermal tolerances for aquatic and terrestrial organisms. *Sci. Data* **5**, 180022 (2018).
47. Bebber, D. P., Ramotowski, M. A. T. & Gurr, S. J. Crop pests and pathogens move polewards in a warming world. *Nat. Clim. Change* **3**, 985–988 (2013).
48. Chaloner, T. M., Gurr, S. J. & Bebber, D. P. Plant pathogen infection risk tracks global crop yields under climate change. *Nat. Clim. Change* **11**, 710–715 (2021).
49. Sloat, L. L. et al. Climate adaptation by crop migration. *Nat. Commun.* **11**, 1243 (2020).
50. Riahi, K. et al. The Shared Socioeconomic Pathways and their energy, land use, and greenhouse gas emissions implications: an overview. *Glob. Environ. Change* **42**, 153–168 (2017).
51. Lambert, F. H. & Chiang, J. C. H. Control of land-ocean temperature contrast by ocean heat uptake. *Geophys. Res. Lett.* **34**, L13704 (2007).
52. Kemp, L. et al. Climate endgame: exploring catastrophic climate change scenarios. *Proc. Natl Acad. Sci. USA* **119**, e2108146119 (2022).
53. Canadell, J. G. et al. in *Climate Change 2021: The Physical Science Basis* (eds Masson-Delmotte, V. et al.) 673–816 (IPCC, Cambridge Univ. Press, 2021).
54. Crippa, M. et al. *Emissions Database for Global Atmospheric Research, Version v6.0_FT_2020 (GHG Time-Series)* (European Commission, Joint Research Centre, 2021); http://data.europa.eu/89h/2f134209-21d9-4b42-871c-58c3bdcfb549
55. Callaghan, M. et al. Machine-learning-based evidence and attribution mapping of 100,000 climate impact studies. *Nat. Clim. Change* **11**, 966–972 (2021).
56. Tuholske, C. et al. Global urban population exposure to extreme heat. *Proc. Natl Acad. Sci. USA* **118**, e2024792118 (2021).
57. Klein, T. & Anderegg, W. R. L. A vast increase in heat exposure in the 21st century is driven by global warming and urban population growth. *Sustain. Cities Soc.* **73**, 103098 (2021).
58. Seneviratne, S. I. et al. in *Climate Change 2021: The Physical Science Basis* (eds Masson-Delmotte, V. et al.) 1513–1766 (IPCC, Cambridge Univ. Press, 2021).
59. Ramage, J. et al. Population living on permafrost in the Arctic. *Popul. Environ.* **43**, 22–38 (2021).
60. McNamara, K. E. & Jackson, G. Loss and damage: a review of the literature and directions for future research. *Wiley Interdiscip. Rev. Clim. Change* **10**, e564 (2019).
61. New, M. et al. in *Climate Change 2022: Impacts, Adaptation and Vulnerability* (eds Pörtner, H.-O. et al.) 2539–2654 (IPCC, Cambridge Univ. Press, 2022).
62. Ameli, N. et al. Higher cost of finance exacerbates a climate investment trap in developing economies. *Nat. Commun.* **12**, 4046 (2021).
63. Klein Goldewijk, K., Beusen, A., Doelman, J. & Stehfest, E. Anthropogenic land use estimates for the Holocene—HYDE 3.2. *Earth Syst. Sci. Data* **9**, 927–953 (2017).
64. Hijmans, R. J., Cameron, S. E., Parra, J. L., Jones, P. G. & Jarvis, A. Very high resolution interpolated climate surfaces for global land areas. *Int. J. Climatol.* **25**, 1965–1978 (2005).
65. Harris, I., Osborn, T. J., Jones, P. & Lister, D. Version 4 of the CRU TS monthly high-resolution gridded multivariate climate dataset. *Sci. Data* **7**, 109 (2020).
66. University of East Anglia Climatic Research Unit; Harris, I. C., Jones, P. D. & Osborn, T. *CRU TS4.05: Climatic Research Unit (CRU) Time-Series (TS) Version 4.05 of High-Resolution Gridded Data of Month-by-Month Variation in Climate (Jan. 1901–Dec. 2020)* (NERC EDS Centre for Environmental Data Analysis, 2021).
67. Rodell, M. et al. The Global Land Data Assimilation System. *Bull. Am. Meteorol. Soc.* **85**, 381–394 (2004).
68. Knox, J. A., Nevius, D. S. & Knox, P. N. Two simple and accurate approximations for wet-bulb temperature in moist conditions, with forecasting applications. *Bull. Am. Meteorol. Soc.* **98**, 1897–1906 (2017).
69. Sandstad, M., Schwingshackl, C., Iles, C. E. & Sillmann, J. *Climate Extreme Indices and Heat Stress Indicators Derived from CMIP6 Global Climate Projections* (Copernicus Climate Change Service Climate Data Store, accessed 26 October 2022); https://doi.org/10.24381/cds.776e08bd
70. Buzan, J. R., Oleson, K. & Huber, M. Implementation and comparison of a suite of heat stress metrics within the Community Land Model version 4.5. *Geosci. Model Dev.* **8**, 151–170 (2015).
71. Muñoz Sabater, J. *ERA5-Land Monthly Averaged Data From 1950 to Present* (Copernicus Climate Change Service Climate Data Store, accessed 3 May 2022); https://doi.org/10.24381/cds.68d2bb30
72. McNally, A. et al. A land data assimilation system for sub-Saharan Africa food and water security applications. *Sci. Data* **4**, 170012 (2017).
73. McNally, A. NASA/GSFC/HSL FLDAS Noah Land Surface Model L4 Global Monthly 0.1 x 0.1 Degree (MERRA-2 and CHIRPS) (Goddard Earth Sciences Data and Information Services Center, accessed 3 May 2022); https://doi.org/10.5067/5NHC22T9375G
74. Saha, S. et al. *NCEP Climate Forecast System Version 2 (CFSv2) 6-Hourly Products* (Research Data Archive at the National Center for Atmospheric Research, Computational and Information Systems Laboratory, 2011).
75. KC, S. & Lutz, W. The human core of the Shared Socioeconomic Pathways: population scenarios by age, sex and level of education for all countries to 2100. *Glob. Environ. Change* **42**, 181–192 (2017).
76. Jones, B. & O'Neill, B. C. Spatially explicit global population scenarios consistent with the Shared Socioeconomic Pathways. *Environ. Res. Lett.* **11**, 084003 (2016).
77. Gao, J. *Downscaling Global Spatial Population Projections from 1/8-Degree to 1-km Grid Cells (No. NCAR/TN-537+STR)* (National Center for Atmospheric Research, Technical Notes, 2017); https://doi.org/10.5065/D60Z721H
78. O'Neill, B. C. et al. A new scenario framework for climate change research: the concept of Shared Socioeconomic Pathways. *Clim. Change* **122**, 387–400 (2014).
79. IPCC in *Climate Change 2021: The Physical Science Basis* (eds Masson-Delmotte, V. et al.) 3–32 (Cambridge Univ. Press, 2021).
80. *Poverty and Inequality Platform* (World Bank, accessed 20 May 2022); https://pip.worldbank.org

Acknowledgements
We thank all the data providers. T.M.L., J.F.A. and A.G. are supported by the Open Society Foundations (OR2021-82956). T.M.L. is supported by a Turing Fellowship. C.X. is supported by the National Key R&D Program of China (2022YFF1301000), the National Natural Science Foundation of China (32061143014) and the Fundamental Research Funds for the Central Universities (9610065). J.-C.S. is supported by VILLUM Investigator project 'Biodiversity Dynamics in a Changing World' funded by VILLUM FONDEN (grant 16549). M.S. is supported by an ERC Advanced Grant and a Spinoza award. This work is part of the Earth Commission, which is hosted by Future Earth and is the science component of the Global Commons Alliance. The Global Commons Alliance is a sponsored project of Rockefeller Philanthropy Advisors, with support from Oak Foundation, MAVA, Porticus, Gordon and Betty Moore Foundation, Herlin Foundation and the Global Environment Facility.

Author contributions
T.M.L., C.X. and M.S. designed the study. C.X. performed the climate niche analyses with input from T.M.L. T.M.L. and J.F.A. related present emissions to future exposure. C.X., J.F.A. and S.L. produced the figures with input from T.M.L., B.S. and C.Z. T.M.L. wrote the paper with input from C.X., J.F.A., A.G., S.L., B.S., C.Z., K.L.E., R.R.D., J.-C.S. and M.S.

Competing interests
The authors declare no competing interests.

Additional information
Extended data is available for this paper at https://doi.org/10.1038/s41893-023-01132-6.

Supplementary information The online version contains supplementary material available at https://doi.org/10.1038/s41893-023-01132-6.

Correspondence and requests for materials should be addressed to Timothy M. Lenton or Chi Xu.

Peer review information *Nature Sustainability* thanks Enrique Martínez-Meyer and the other, anonymous, reviewers for their contribution to the peer review of this work.

https://doi.org/10.1038/s41893-023-01132-6

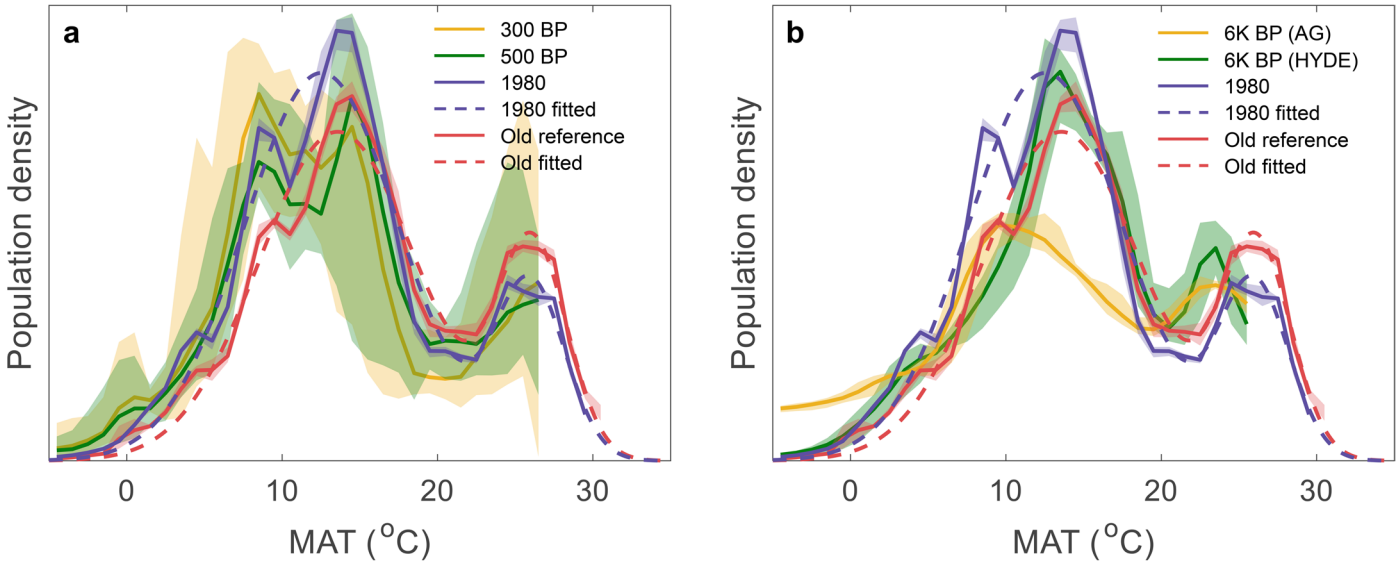

Extended Data Fig. 1 | Relative human population density with respect to Mean Annual Temperature (MAT). Reconstructions from ref. 14. for **a**. 300 BP, 500 BP (population data from HYDE database), and **b**. 6000 BP with population data from ArchaeoGlobe (AG) or HYDE, compared to the 1960-1990 climate (~0.3 °C above pre-industrial) with 2015 population distribution ('Old reference', from ref. 14) or 1980 population distribution ('1980', used here; as in Fig. 1a), and the smooth fitted functions for the temperature niche used previously[14] ('Old fitted') and here ('1980 fitted'; as in Fig. 1a) for future projections. Data presented as mean values with the shaded regions corresponding to 5-95th percentiles. Truncation of the historical reconstructions at higher temperatures is due to excluding bins of data with too few points in them to avoid outlier effects (see ref. 14).

https://doi.org/10.1038/s41893-023-01132-6

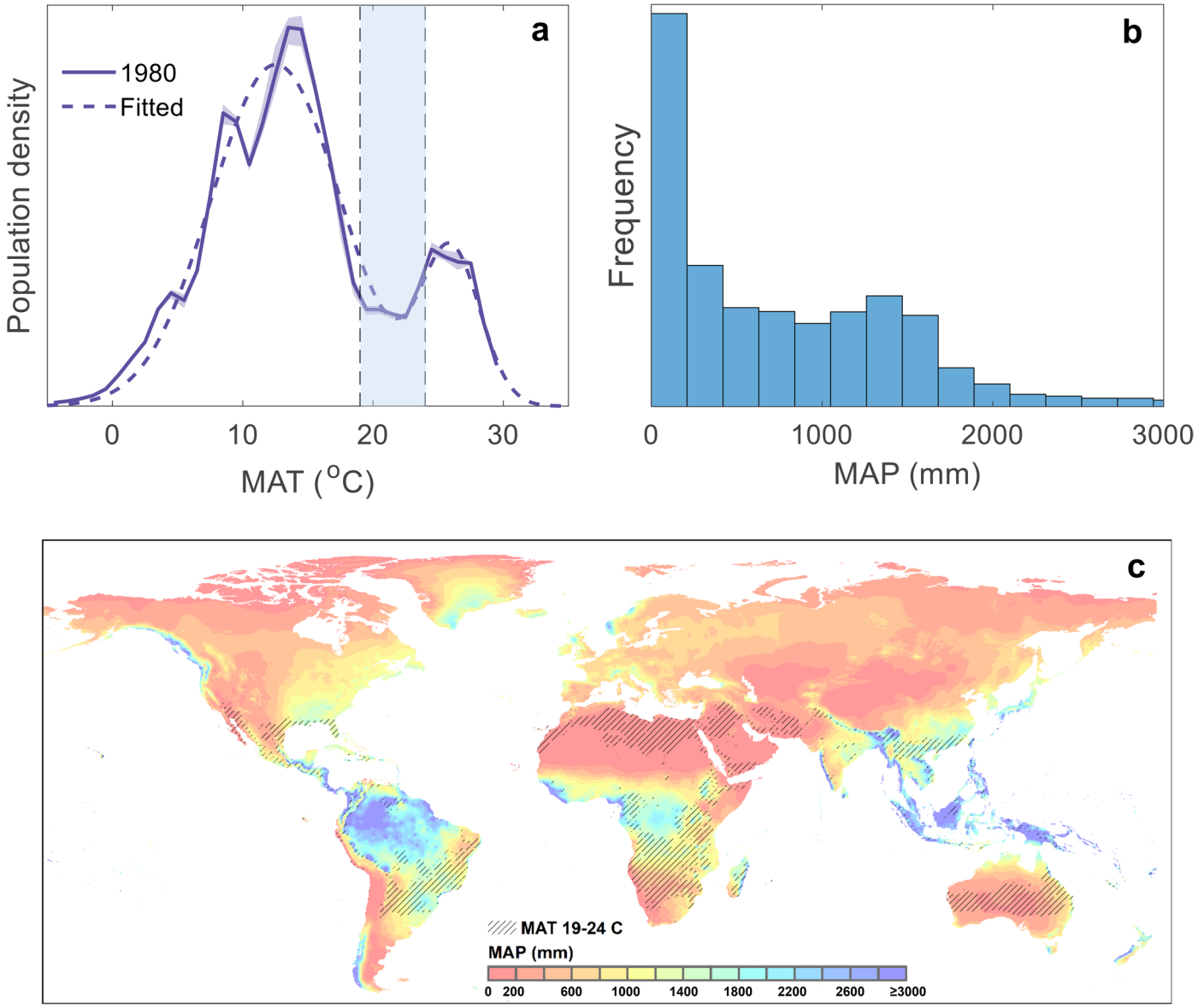

Extended Data Fig. 2 | Association of the temperature niche minimum with drier climates. a. The temperature niche has relatively low population density between 19 °C and 24 °C (blue vertical band). Data for 1980 presented as mean values with the shaded regions corresponding to 5-95th percentiles. **b**. Frequency distribution of mean annual precipitation (MAP) in the 19-24 °C MAT regions. **c**. Map of mean annual precipitation with the 19-24 °C MAT regions overlaid (cross hatching) showing they include large areas of deserts.

https://doi.org/10.1038/s41893-023-01132-6

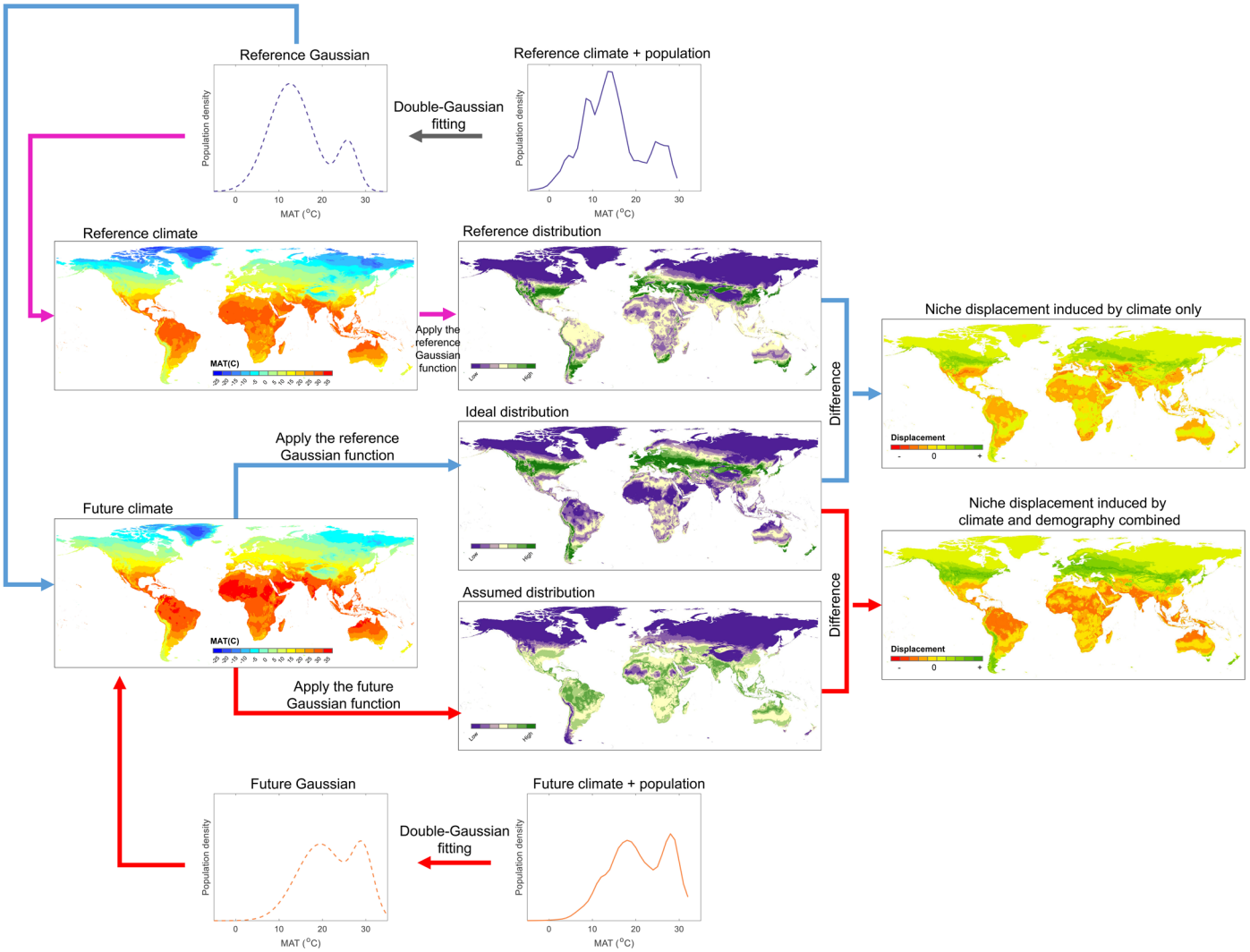

Extended Data Fig. 3 | Workflow for quantifying displacement of the human climate niche due to climate change only or climate and demographic change. Workflow shown for the temperature niche (but the same approach is used for the temperature-precipitation niche).

https://doi.org/10.1038/s41893-023-01132-6

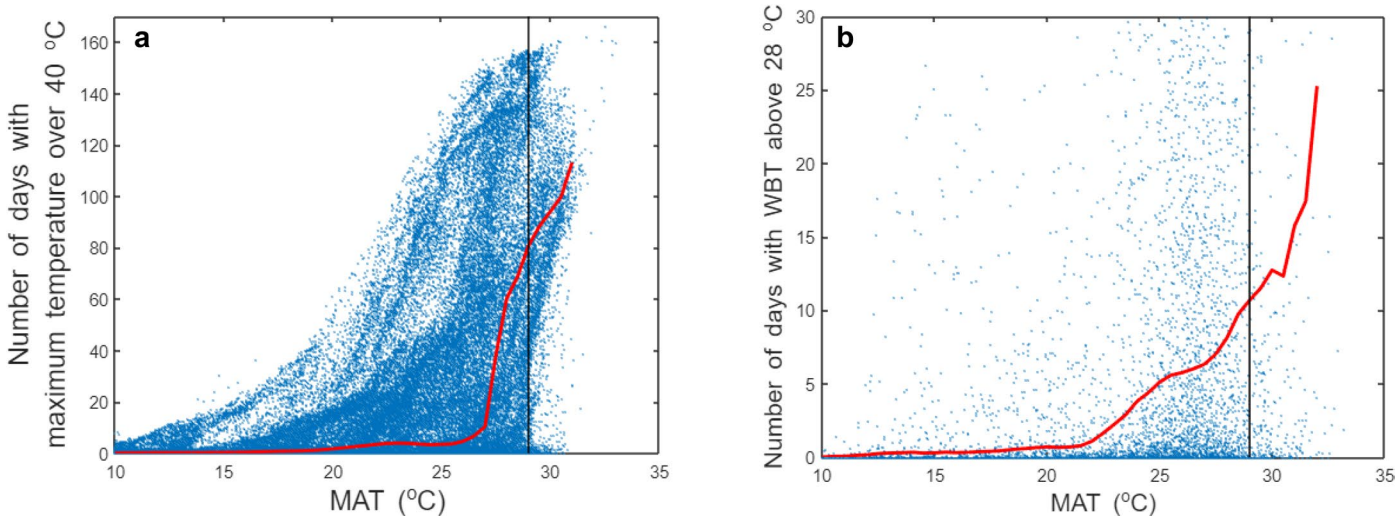

Extended Data Fig. 4 | Relationships between mean annual temperature (MAT) and accumulated intolerable heat extremes (for 2000-2020). **a**. Number of days with maximum temperature above 40 °C calculated using ERA5 data (10 km spatial resolution, n = 2287025). **b**. Number of days with maximum wet bulb temperature (WBT) above 28 °C calculated using bias corrected data from an ensemble of six CMIP6 models (2.8° spatial resolution, n = 49152). Red curves represent running means (with a bin width of 2 °C and step of 0.5 °C); black vertical lines mark 29 °C MAT. See Methods for further details of models and calculations.

https://doi.org/10.1038/s41893-023-01132-6

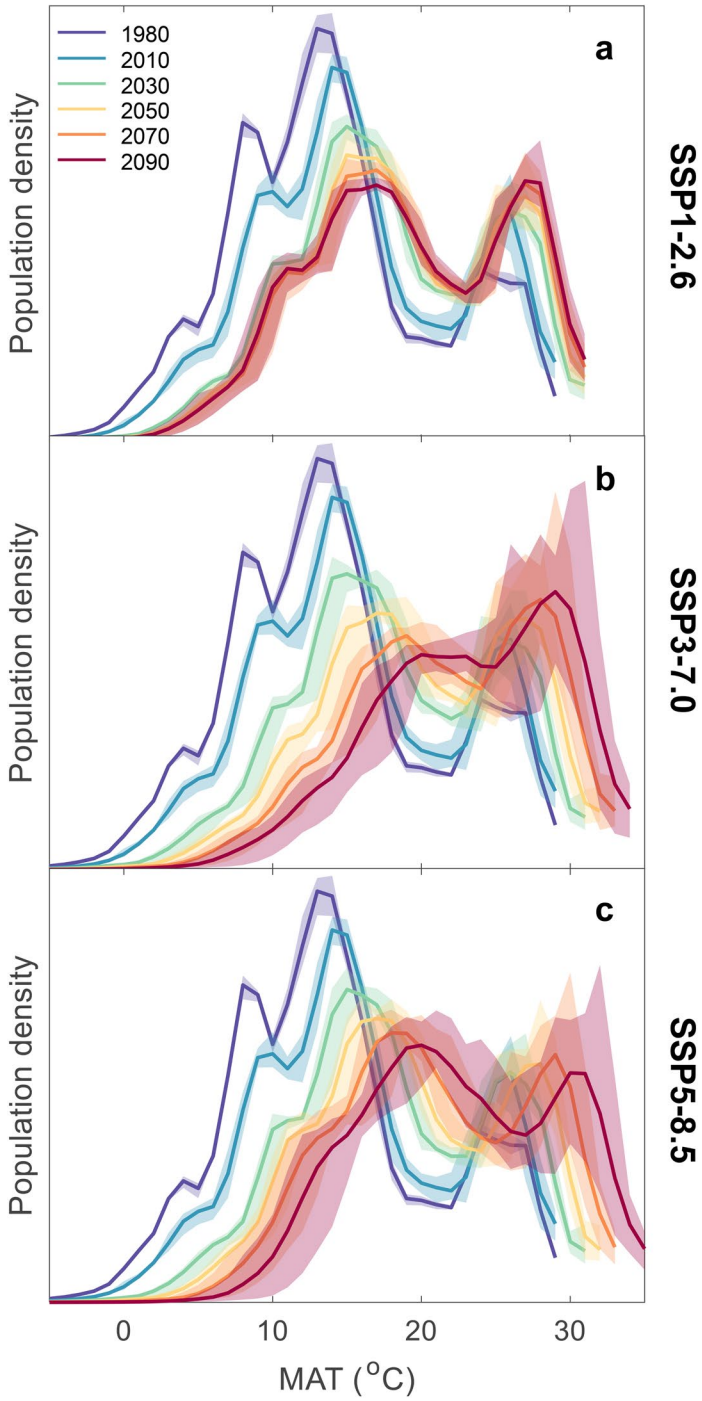

Extended Data Fig. 5 | Observed and projected future changes in human population density with respect to Mean Annual Temperature (MAT), following different Shared Socio-economic Pathways (SSPs). a. SSP1-2.6 leading to ~1.8 °C global warming with a peak of 8.5 billion people. **b**. SSP3-7.0 scenario leading to ~3.6 °C global warming and 12.1 billion people. **c**. SSP5-8.5 scenario leading to ~4.4 °C global warming and a peak of 8.6 billion people. (The SSP2-4.5 scenario is shown in Fig. 1b.) For each SSP and 20-year averaged climate interval, global warming and corresponding population levels (for the central year) are summarized in Extended Data Table 1. Data presented as mean values with the shaded regions corresponding to 5-95th percentiles.

https://doi.org/10.1038/s41893-023-01132-6

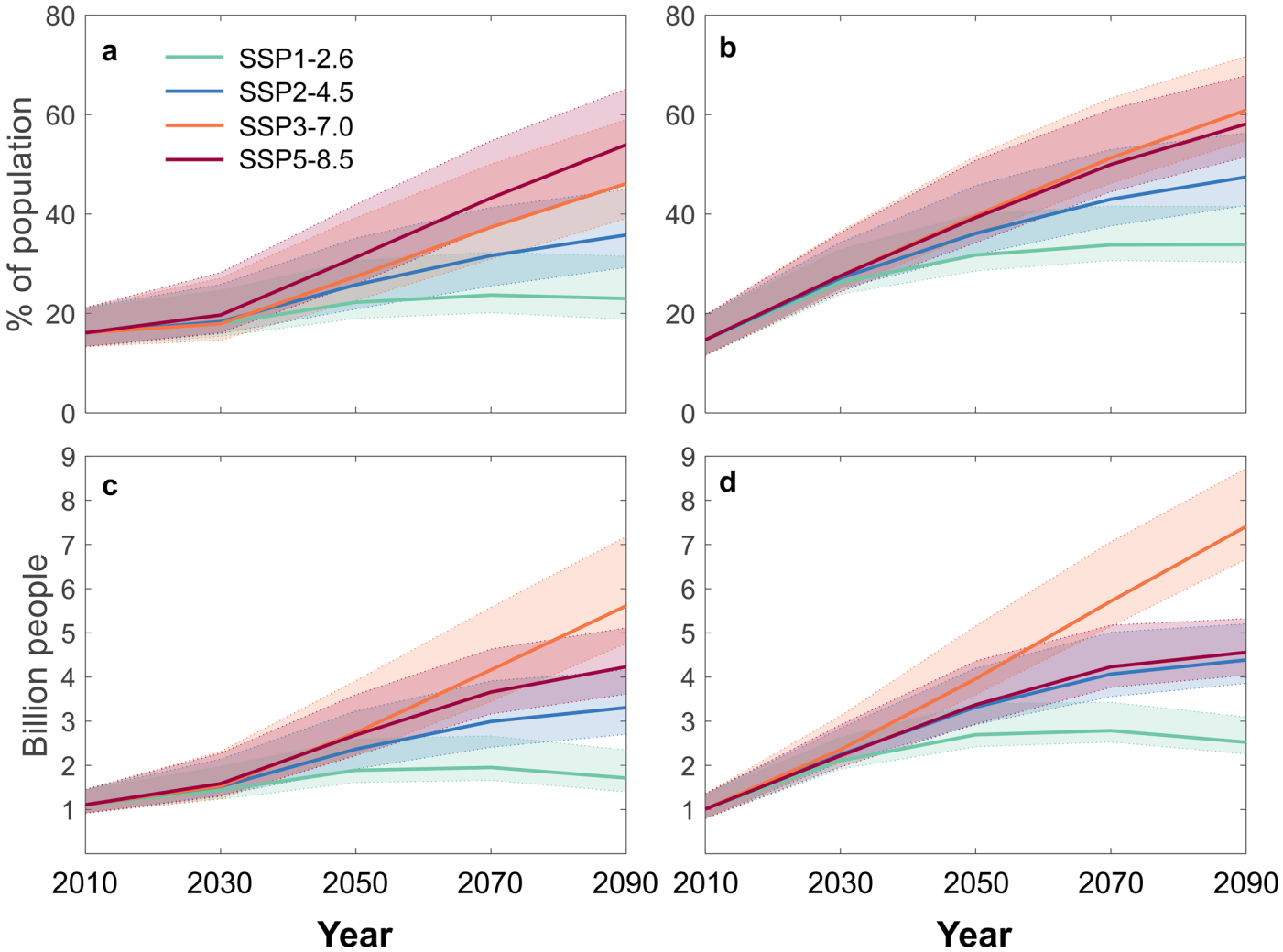

Extended Data Fig. 6 | Population exposed outside of the temperature-precipitation niche, following different Shared Socio-economic Pathways (SSPs). a, b. Fraction of population (%) left outside of the niche due to: **a.** climate change only. **b.** climate and demographic change. **c, d.** Absolute number left outside of the niche due to: **c.** climate change only. **d.** climate and demographic change. Calculations based on mean annual temperature (MAT) and precipitation (MAP) averaged over the 20-year intervals and population density distribution at the centre year of the corresponding intervals. Data presented as mean values with the shaded regions corresponding to 5-95th percentiles. (Note that the population exposed to unprecedented hot MAT ≥ 29 °C is unaltered by considering precipitation changes).

https://doi.org/10.1038/s41893-023-01132-6

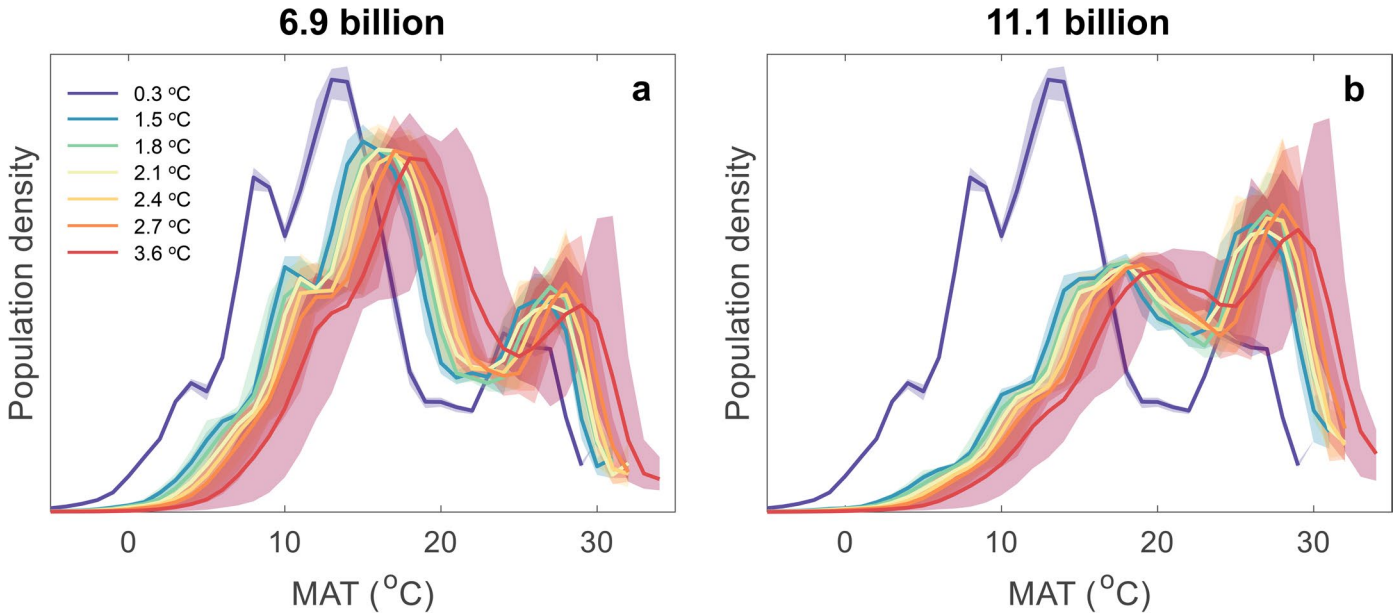

Extended Data Fig. 7 | Changes in human population density with respect to Mean Annual Temperature (MAT) for different fixed population distributions and levels of global warming. The population distributions are: **a**. 6.9 billion in 2010, **b**. 11.1 billion under SSP3 in 2070 (9.5 billion under SSP2 in 2070 is shown in Fig. 1c). See Methods for the combinations of SSP and 20-year time interval representing different global warming levels. Data presented as mean values with the shaded regions corresponding to 5-95th percentiles.

https://doi.org/10.1038/s41893-023-01132-6

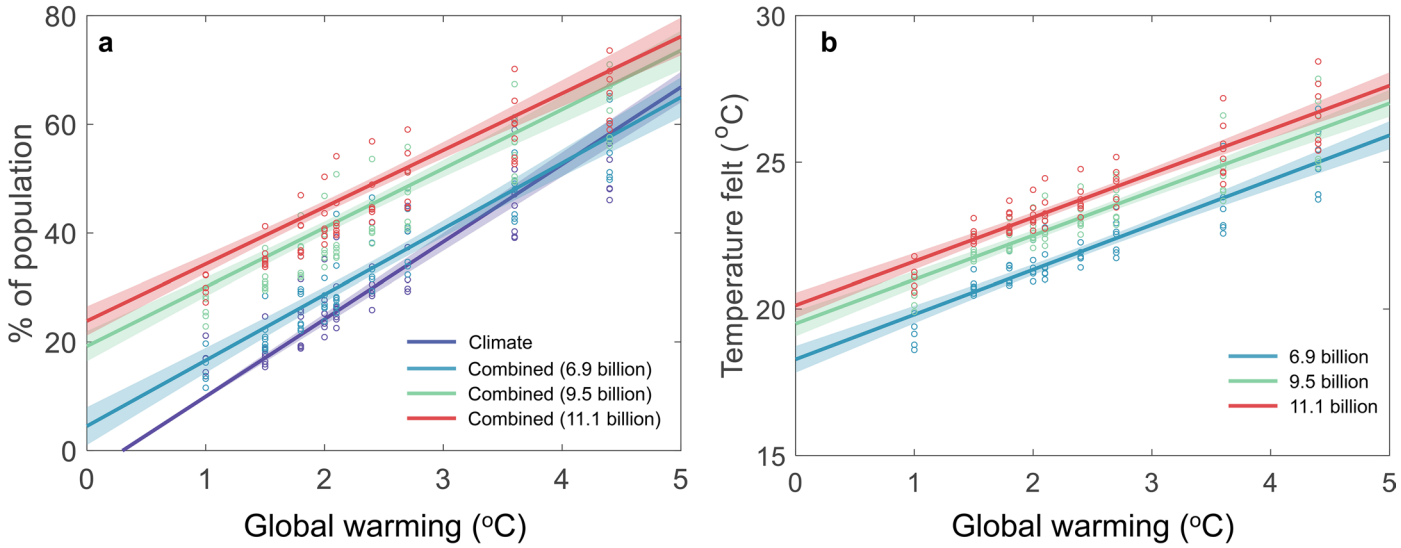

Extended Data Fig. 8 | Relationships between global warming and temperature-precipitation niche displacement and between global warming and average temperature experienced. a. Near linear relationship between global warming and temperature-precipitation niche displacement (%) due to temperature and precipitation change only ('Climate') and due to climate plus demographic change ('Combined'). Linear regression results: Climate (n = 65, coefficient=14.2 % °C^{-1}; forcing intercept at 1960-1990 global warming of 0.3 °C); Combined 6.9 billion (n = 65, coefficient=12.0 % °C^{-1}, r^2 = 0.84); Combined 9.5 billion (n = 65, coefficient=10.9 % °C^{-1}, r^2 = 0.84); Combined 11.1 billion (n = 65, coefficient=10.5 % °C^{-1}, r^2 = 0.84). **b**. Mean annual temperature felt by an average person for different levels of global warming for fixed population distributions. Linear regression results: 6.9 billion (n = 65, coefficient=1.53 °C °C^{-1}, r^2 = 0.83); 9.5 billion (n = 65, coefficient=1.50 °C °C^{-1}, r^2 = 0.84); 11.1 billion (n = 65, coefficient=1.50 °C °C^{-1}, r^2 = 0.84). The shaded regions correspond to 95% two-sided confidence intervals of the estimated regression coefficients.

https://doi.org/10.1038/s41893-023-01132-6

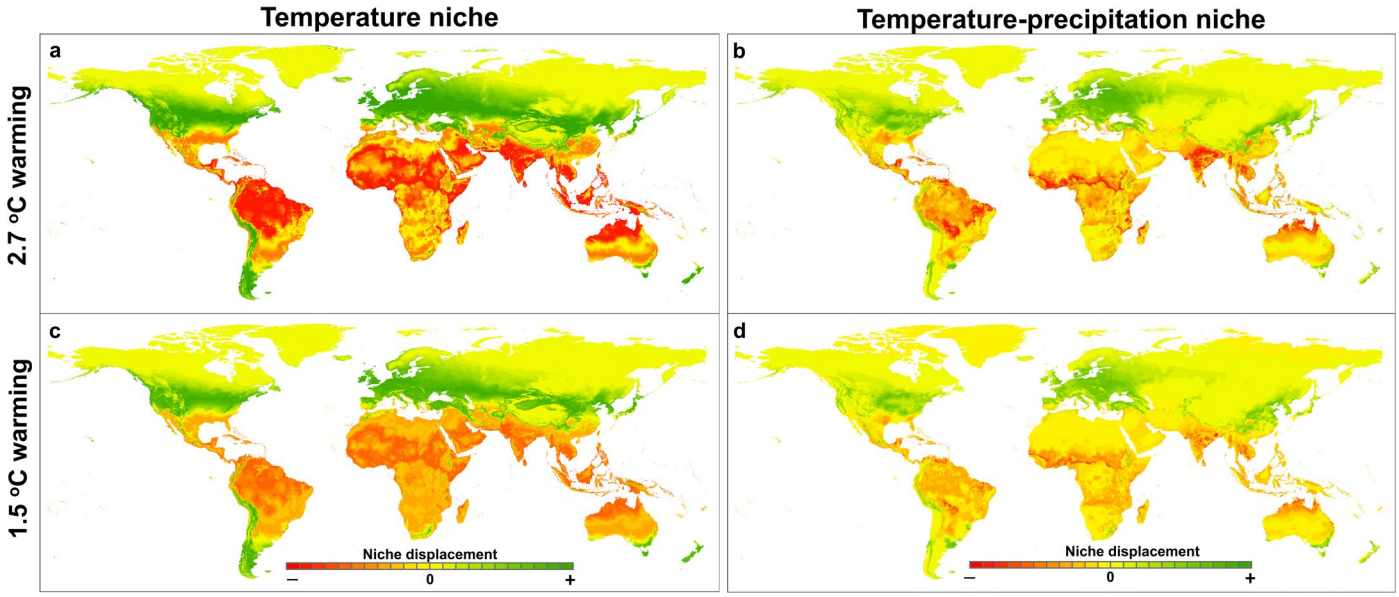

Extended Data Fig. 9 | Displacement of the temperature and temperature-precipitation niches under different levels of global warming. a, b. 2.7 °C global warming due to current policies, **c, d.** 1.5 °C global warming meeting the Paris Agreement. Red indicates a decrease in suitability, green an increase. Note that the less extensive changes in the temperature-precipitation niche are because it already constrains population density more in the driest and wettest regions.

https://doi.org/10.1038/s41893-023-01132-6

Extended Data Table 1 | Global warming and world population levels for each Shared Socioeconomic Pathway (SSP)

	Scenario	2020-2040	2040-2060		2080-2100
Warming (°C)	SSP1-2.6	1.5 (1.2-1.8)	1.7 (1.3-2.2)		1.8 (1.3-2.4)
	SSP2-4.5	1.5 (1.2-1.8)	2.0 (1.6-2.5)		2.7 (2.1-3.5)
	SSP3-7.0	1.5 (1.2-1.8)	2.1 (1.7-2.6)		3.6 (2.8-4.6)
	SSP5-8.5	1.6 (1.3-1.9)	2.4 (1.9-3.0)		4.4 (3.3-5.7)
	Scenario	**2030**	**2050**	**2070**	**2090**
World total Population (billion)	SSP1	8.0	8.5	8.2	7.4
	SSP2	8.3	9.2	9.5	9.2
	SSP3	8.5	9.9	11.1	12.1
	SSP5	8.0	8.6	8.4	7.8

Global warming levels are the 20-year averages from the full CMIP6 ensemble (Table SPM.1 of IPCC AR6 WG1). World population levels are given for the central year of each 20-year interval.

nature research

Corresponding author(s): Timothy M. Lenton, Chi Xu

Last updated by author(s): Apr 18, 2023

Reporting Summary

Nature Research wishes to improve the reproducibility of the work that we publish. This form provides structure for consistency and transparency in reporting. For further information on Nature Research policies, see our Editorial Policies and the Editorial Policy Checklist.

Statistics

For all statistical analyses, confirm that the following items are present in the figure legend, table legend, main text, or Methods section.

n/a	Confirmed	
☐	☒	The exact sample size (*n*) for each experimental group/condition, given as a discrete number and unit of measurement
☒	☐	A statement on whether measurements were taken from distinct samples or whether the same sample was measured repeatedly
☐	☒	The statistical test(s) used AND whether they are one- or two-sided *Only common tests should be described solely by name; describe more complex techniques in the Methods section.*
☒	☐	A description of all covariates tested
☒	☐	A description of any assumptions or corrections, such as tests of normality and adjustment for multiple comparisons
☐	☒	A full description of the statistical parameters including central tendency (e.g. means) or other basic estimates (e.g. regression coefficient) AND variation (e.g. standard deviation) or associated estimates of uncertainty (e.g. confidence intervals)
☐	☒	For null hypothesis testing, the test statistic (e.g. *F*, *t*, *r*) with confidence intervals, effect sizes, degrees of freedom and *P* value noted *Give P values as exact values whenever suitable.*
☒	☐	For Bayesian analysis, information on the choice of priors and Markov chain Monte Carlo settings
☒	☐	For hierarchical and complex designs, identification of the appropriate level for tests and full reporting of outcomes
☒	☐	Estimates of effect sizes (e.g. Cohen's *d*, Pearson's *r*), indicating how they were calculated

Our web collection on statistics for biologists contains articles on many of the points above.

Software and code

Policy information about availability of computer code

Data collection	The publicly available cloud computation platform Google Earth Engine was used for the collection of the NASA GLDAS-2.1 data, the ECMWF ERA5 data, the NASA FLDAS data, and the NCEP CFSV2 data.
Data analysis	Code used for the analysis is available from https://doi.org/10.6084/m9.figshare.22650760.v1.

For manuscripts utilizing custom algorithms or software that are central to the research but not yet described in published literature, software must be made available to editors and reviewers. We strongly encourage code deposition in a community repository (e.g. GitHub). See the Nature Research guidelines for submitting code & software for further information.

Data

Policy information about availability of data

All manuscripts must include a data availability statement. This statement should provide the following information, where applicable:

- Accession codes, unique identifiers, or web links for publicly available datasets
- A list of figures that have associated raw data
- A description of any restrictions on data availability

The historical and current population distribution data are available from the HYDE 3.2 database at https://landuse.sites.uu.nl/datasets/. The WorldClim v1.4 data are available at https://doi.org/10.5061/dryad.fj6q573q7. The CRU TS v.4.05 and v.4.06 monthly data are available at https://crudata.uea.ac.uk/cru/data/hrg/. The NASA GLDAS-2.1 3-hourly data are available at https://developers.google.com/earth-engine/datasets/catalog/NASA_GLDAS_V021_NOAH_G025_T3H. The ECMWF ERA5 daily data are available at https://developers.google.com/earth-engine/datasets/catalog/ECMWF_ERA5_DAILY. The bias-corrected wet bulb temperature data are available at https://cds.climate.copernicus.eu/cdsapp#!/dataset/sis-extreme-indices-cmip6. The ECMWF ERA5-Land monthly data are available at https://developers.google.com/earth-engine/datasets/catalog/ECMWF_ERA5_LAND_MONTHLY. The NASA FLDAS monthly data are available at https://developers.google.com/earth-engine/datasets/catalog/NASA_FLDAS_NOAH01_C_GL_M_V001. The NCEP CFSV2 6-hourly data are available at https://

developers.google.com/earth-engine/datasets/catalog/NOAA_CFSV2_FOR6H. The downscaled CMIP6 climate data are available from WorldClim v2.0 at https://worldclim.org. The SSP population projection data are available at https://www.cgd.ucar.edu/iam/modeling/spatial-population-scenarios.html. The GIS data for country boundaries from the World Borders Dataset are available at https://thematicmapping.org/downloads/world_borders.php. The poverty data for 2019 from the World Bank's Poverty and Inequality Platform are available at https://pip.worldbank.org/home. All data generated during this study are available from https://doi.org/10.6084/m9.figshare.22650361.v1.

Field-specific reporting

Please select the one below that is the best fit for your research. If you are not sure, read the appropriate sections before making your selection.

☐ Life sciences ☐ Behavioural & social sciences ☒ Ecological, evolutionary & environmental sciences

For a reference copy of the document with all sections, see nature.com/documents/nr-reporting-summary-flat.pdf

Ecological, evolutionary & environmental sciences study design

All studies must disclose on these points even when the disclosure is negative.

Study description	A data and model output based study of the distribution of human population density with respect to mean annual temperature and precipitation up to present and under future projections, with additional analyses of country-level exposure.
Research sample	No research sample in the sense described (all people on the planet considered in the analysis).
Sampling strategy	No corresponding sampling strategy.
Data collection	Data obtained by Chi Xu from public datasets for human population and climate scenarios.
Timing and spatial scale	Timing of data collection not relevant as the data sources already existed and are archived.
Data exclusions	No data were excluded from the analyses
Reproducibility	No experiments were undertaken
Randomization	No allocation into groups as this is a global analysis
Blinding	Blinding not relevant as global analysis

Did the study involve field work? ☐ Yes ☒ No

Reporting for specific materials, systems and methods

We require information from authors about some types of materials, experimental systems and methods used in many studies. Here, indicate whether each material, system or method listed is relevant to your study. If you are not sure if a list item applies to your research, read the appropriate section before selecting a response.

Materials & experimental systems

n/a	Involved in the study
☒	☐ Antibodies
☒	☐ Eukaryotic cell lines
☒	☐ Palaeontology and archaeology
☒	☐ Animals and other organisms
☒	☐ Human research participants
☒	☐ Clinical data
☒	☐ Dual use research of concern

Methods

n/a	Involved in the study
☒	☐ ChIP-seq
☒	☐ Flow cytometry
☒	☐ MRI-based neuroimaging